IEEE Journal of Microwaves

Received 3 April 2023; revised 12 May 2023; accepted 13 May 2023. Date of publication 22 June 2023; date of current version 7 July 2023.

Digital Object Identifier 10.1109/JMW.2023.3278237

Towards Continuous Real-Time Plant and Insect Monitoring by Miniaturized THz Systems

FAWAD SHEIKH [1] (Member, IEEE), ANDREAS PROKSCHA [1] (Graduate Student Member, IEEE), AMAN BATRA [1], DIEN LESSY [1] (Graduate Student Member, IEEE), BAHA SALAH [1] (Graduate Student Member, IEEE), BENEDIKT SIEVERT [2] (Member, IEEE), MARVIN DEGEN [2], ANDREAS RENNINGS [2] (Member, IEEE), MANDANA JALALI [2], JAN TARO SVEJDA [2] (Member, IEEE), POOYA ALIBEIGLOO [3] (Graduate Student Member, IEEE), CHRISTIAN PREUSS [3], ENES MUTLU [3] (Graduate Student Member, IEEE), ROBIN KRESS [3] (Graduate Student Member, IEEE), SIMONE CLOCHIATTI [3], KEVIN KOLPATZECK [4], TOBIAS KUBICZEK [4], INGRID ULLMANN [5] (Member, IEEE), KONSTANTIN ROOT [5], FABIAN BRIX [6], UTE KRÄMER [6], MARTIN VOSSIEK [5] (Fellow, IEEE), JAN C. BALZER [4] (Member, IEEE), NILS G. WEIMANN [3] (Member, IEEE), THOMAS KAISER [1] (Senior Member, IEEE), AND DANIEL ERNI [2] (Member, IEEE)

(Regular Paper)

[1]Institute of Digital Signal Processing (DSV), University of Duisburg-Essen (UDE), D-47057 Duisburg, Germany
[2]General and Theoretical Electrical Engineering (ATE), Faculty of Engineering, and CENIDE – Center for Nanointegration Duisburg-Essen, University of Duisburg-Essen, D-47048 Duisburg, Germany
[3]Department High Frequency Electronic Components (BHE), CENIDE – Center for Nanointegration Duisburg-Essen, University of Duisburg-Essen, D-47048 Duisburg, Germany
[4]Chair of Communication Systems (NTS), University of Duisburg-Essen, D-47057 Duisburg, Germany
[5]Institute of Microwaves and Photonics (LHFT), Friedrich-Alexander-Universität Erlangen-Nürnberg, D-91058 Erlangen, Germany
[6]Institute of Molecular Genetics and Physiology of Plants (MGPP), Ruhr University Bochum, D-44801 Bochum, Germany

CORRESPONDING AUTHOR: Fawad Sheikh (e-mail: fawad.sheikh@uni-due.de).

This work was supported in part by the Deutsche Forschungsgemeinschaft through TRR 196 MARIE Projects M01, M03, M05, C02, C05, S01, S03 and S05, under Grant Project-ID 287022738, in part by the Ministry of Culture and Science of the State of North Rhine-Westphalia (MKW NRW) through Project terahertz.NRW, in part by the German Federal Ministry of Education and Research (BMBF) in the course of the 6GEM Research Hub under Grant 16KISK038, in part by the EU and the State of North Rhine Westfalia through Project "Terahertz-Integrationszentrum (THzIZ)", under Grant EFRE-0400215, and in part by the Open Access Publication Fund of the University of Duisburg-Essen. The project terahertz.NRW was supported by the program Netzwerke 2021, an initiative of the Ministry of Culture and Science of the State of Northrhine Westphalia.

ABSTRACT In this paper, new concepts for continuous 24/7 real-time monitoring of plants and insects with miniaturized terahertz (THz) systems are described and experimentally tested. Thus, for the first time, small-scale insights into the instantaneous plant health but also in their long-term growth can be obtained. Using such compact THz systems, e.g. water uptake, insect infestation and the behavior of pollinators (i.e. honey bees) and pests can be measured dynamically and non-invasively at virtually any position in the close biotope surrounding them. In addition to general understanding, this can be used to optimize crop yield and reduce resource consumption as well as for identifying characteristics of insect-plant interactions induced by potential environmental stressors. Given such a holistic approach, the proposed concepts may provide a significant advancement in environmental monitoring technology.

INDEX TERMS 24/7 insect tracking, 24/7 plant monitoring, finite element method (FEM), millimeter wave multiple-input multiple-output (MIMO) radar, photorealistic ray-tracing, radar cross-section (RCS), recursive aggregated T-matrix algorithm, resonant tunneling diode (RTD) detector, specific absorption rate, surface roughness, synthetic aperture radar (SAR), THz measurements and simulations, THz time domain spectroscopy (THz-TDS), THz-VNA testbed.

I. INTRODUCTION

Fabian Brix, Ute Krämer, Fawad Sheikh, Andreas Prokscha, Martin Vossiek, Jan C. Balzer, Nils G. Weimann, Thomas Kaiser, Daniel Erni

A. ACCESSING CLOSE MODEL ECOSYSTEMS

The responses of central model plants to individual biotic and abiotic environmental factors have been well characterized in standardized growth chamber or greenhouse environments at the morphological, physiological, biochemical and molecular levels. Work in recent years has highlighted that simulating natural fluctuations in environmental conditions, in particular light intensity [1], [2], [3], as well as the combination of impacts from several environmental factors [4], [5], [6], [7] can trigger fundamentally different responses in plants that are more and more in the focus of current research in the plant sciences. These studies, although highly insightful and of critical importance, only move us one step further towards the ultimate new frontier in phenomics: Multi-level monitoring of the ecological interactions between plants and their environments in natural habitats and in agricultural fields. Technological advances towards miniaturization and an expanded scope of sensing devices as well as increasing options and volumes for data transfer and collection [8], [9], [10], [11] will progressively allow to approach this new frontier in the future. Here we outline our long-term vision, provide the results of some initial measurements using simple model systems employing current state-of-the art methodology, and we specify the upcoming set of objectives towards our longer-term vision.

Our long-term vision is as follows: It would be desirable to simultaneously and continuously monitor during daytime and nighttime for a number of individual plants in the field (1) representative parameters describing the abiotic microenvironment, (2) output parameters and/or even reporters of plant physiological health status and plant performance, as well as (3) the number and activities of organisms interacting with the plant. In relation to (1), it is desirable to monitor light/radiation intensity and quality, air composition and humidity, air temperature, as well as soil humidity, temperature and ideally the composition and the pH of the soil solution in the immediate vicinity of the roots of the plant. With respect to (2), it is desirable to qualitatively and quantitatively monitor plant biomass gain above and below ground, flowering, seed set, leaf water content, gas exchange and water loss across the leaf surface, leaf surface temperature and ideally also the composition of leaves with respect to nutrient and non-nutrient elements, for example toxic heavy metals, as well as contents in major organic compounds such as photoassimilates and major groups of secondary metabolites.

As an expanded set of plant parameters, it would be insightful to monitor the spectrum and quantities of volatiles emitted from the leaves, for example ethylene, terpenes and volatile forms of jasmonate, oxylipins and salicylate, for example. Finally, in relation to (3), relevant biotic factors are microorganisms, herbivores and pollinators, as well as neighboring plants. As a first goal, we envisage to count in a localized manner both the visits and numbers of insects and other small animals present on the plant, identify their types and activities of insects (e.g. leaf consumption, sucking), be able to count how many insects are on the plant, and what do they do (eat, suck). For now, we envisage update rates in the order of one minute overall.

FIGURE 1. Example of an envisioned environment for monitoring plants and insects.

Accomplishing this would allow to monitor plant performance and responses, as well as their interactions with the environment, in natural ecological settings. This would provide access to ecologically more relevant phenotypes, for example, as well as a wealth of ecological and mechanistic insights. Specifically, we plan to address in case studies in the field, for example, how dynamics and between-plant variation in leaf composition relate to plant attractiveness for or deterrence of herbivory. Combined with high-throughput technologies such as next-generation sequencing, such comprehensive monitoring could be employed to identify molecular mechanisms and the genetic basis of newly identified phenotypes in an ecological context. This could have enormous potential for fundamental insights into plant biology and towards crop protection and the breeding of more resilient crops. At present, the analysis of responses to environmental factors is generally limited to standardized indoor settings and experimental designs in which plant responses or health parameters are assessed destructively at pre-defined time points, which may or might not be ecologically relevant. Ecological experiments presently depend to a large extent on manual work, such as trapping and counting of insects, or collection and ex situ analysis of soil and leaf samples, for example.

B. MINIATURIZED THZ MONITORING SYSTEMS

The ultimate goal is to develop miniaturized terahertz (THz) systems that can aid in environmental monitoring of biotopes, as depicted in Fig. 1, encompassing various aspects such as assessing the health of plants, detecting insect populations and species, and tracking applications for pollinators, among others. This technology could potentially replace the current method of observation, which relies on human eyesight or camera capture.

In particular at THz frequencies, our holistic approach can provide a new multidimensional paradigm for plant and insect monitoring, as its radical miniaturization program (made possible only by THz operating frequencies) enables ultra-high mobility for tiny, rugged, imperceptible sensors and agile radar imaging systems, their dispersion or positioning at any observation point in the biotope for pinpoint respective stochastic status or continuous life cycle monitoring, together with precise localization and material characterization capabilities.

Systems based on optical sensing have already shown great potential for automatic insect counting and even allowed discrimination between female and male mosquitoes [12]. The accuracy of these systems has been further increased by considering additionally the spectral and time-domain [13]. However, such systems rely on active illumination within the optical band in a well-defined environment and are therefore only available as traps, which clearly contradicts the idea of imperceptible monitoring. Lidar systems are discussed for field measurements without traps. They can cover a large range of more than 100 m but require bulky optics and lasers with several watts of output power, which is dangerous for humans and insects [14]. In contrast, radar systems have shown that insect trajectories can be determined directly in the field by simple means without further measures [15] and that it is in principle possible to classify insects based on the radar cross-section (RCS) [16]. However, these experiments have so far only been performed at frequencies $<$100 GHz, which makes the detection and classification of small insects rather impossible. Therefore, radars that extend into the THz frequency range (100 GHz$-$10 THz) are needed to realize the full potential of insect surveillance in the field.

We shall now focus on our lines of research towards THz plant and insect monitoring, with a specific emphasis on the characteristic interactions between model plants and their interacting small organisms such as pollinators and pests in their immediate ecosystem, particularly in polluted environments. While our vision is broad, we will provide a report on the currently operational THz devices, imaging and sensing techniques, experimental evidence, and modelling efforts that successfully cover all initial activities of our collaborative research program in THz metrology for continuously observing local ecosystems.

The remainder of the paper is organized as follows: Starting with THz plant monitoring in Section II, a first report is given on the development of ultra-compact InGaAs resonant-tunneling diode (RTD)-based THz sources and detectors together with a proof-of-concept for water content detection in a Geranium leaf at 330$-$500 GHz. Section III describes a methodology to estimate internal compartments – and in particular real-time nutrient flows – in plant stems using RCS measurements in conjunction with ultra-fast electromagnetic (EM) inverse problem solvers, where a first successful test has been carried out on a microfluidic 3D-printed stem model for a frequency range of 110$-$170 GHz. Moving further to monitoring scenarios encompassing plants and insects, Section IV studies high-resolution THz synthetic aperture radar (SAR) imaging at 330$-$500 GHz for distinguishing healthy from infested Geranium leaves. The latter are loaded with tiny static insects like aphids or with immobilized honeybees together with eggs of blow flies. Dynamic imaging is addressed in Section V using a 94 x 94 multiple-input multiple-output (MIMO) radar system operating within the E band to successfully track a moving ladybug on a considerably reflecting leaf. In Section VI, a first experimental account is given to THz insect monitoring using THz time-domain spectroscopy (TDS) up to 4 THz within a bi-static setup for the precise RCS estimation and imaging of European honey bees. THz-TDS (up to 2 THz) is also used in Section VII for preparatory channel measurements into a bee hive for future queen bee tracking in e.g. a mating box using a THz harmonic radar. Section VIII analyzes the interaction of THz radiation with honey bees along their digital twins to simulate precise RCSs as well as the EM energy intake for a future detailed EM microdosimetry. In Section IX, we extend the EM model to encompass the immediate surroundings through the use of 3D photorealistic THz ray-tracing simulations, with a particular focus on insect monitoring. As an exemplary numerical benchmark problem, we showcase the ability to remotely detect the micro motions of Varroa mites on the body surface of honey bees, highlighting the impressive capabilities of our approach. A comprehensive conclusion and outlook referring to all discussed activities are provided in Section X.

II. MINIATURIZED THZ CHIPS FOR WATER CONTENT MONITORING

Pooya Alibeigloo, Christian Preuss, Enes Mutlu, Robin Kress, Simone Clochiatti, Nils Weimann

A. ELECTRONIC SIGNAL GENERATION AT THZ FREQUENCIES

THz technology for practical applications in open environments requires a small form factor for system integration and mobility, power efficiency, and robustness, which can be achieved with electronic systems [17]. Commercial electronic THz mixers (frequency extenders) rely on discrete, waveguide-integrated GaAs Schottky diodes [18] and exhibit high performance but are bulky and too expensive for industrial use. Electronic THz integrated circuits have shown strong progress in recent years, with the evolution from simple source and detector components to chips enabling imaging, radar, and other complex functions. Besides ICs made in advanced SiGe and RF-CMOS transistor technologies, III-V semiconductor devices, based on indium phosphide (InP) and related materials, comprising heterojunction bipolar transistors, high electron mobility transistors, and RTD leverage this material systems' advantageous material properties to further extend electronic chip performance in terms of power efficiency and maximum output power at THz frequencies.

B. RESONANT TUNNELING DIODE SOURCES

To overcome the cutoff frequency limit of transistor devices, electron tunneling structures provide an alternative. In these devices, the resistive load of antenna and resonator is cancelled by a negative differential resistance, which occurs through the parallel addition of a tunneling current to the classical thermionic diode current. The RTD is currently the highest frequency electronic oscillator with oscillation frequency of almost 2 THz at room temperature, as demonstrated in several studies [19], [20], [21], [22]. At THz frequencies, i.e. beyond f_{max} of transistors, RTDs offer better DC-to-RF efficiency since they operate as a fundamental oscillator even at these frequencies. The RTD consists of an epitaxially grown III/V compound semiconductor heterostructure. An InGaAs quantum well is sandwiched between two wide-bandgap InAlAs barriers. The layers in the RTD structures are very thin, with thicknesses ranging from 1 nm to 5 nm, allowing for ultra-fast electronic tunneling and thus short transit time [23].

When an RTD is biased to a specific level, the energy level in the quantum well is in resonance with the emitter, resulting in a tunneling current through device. However, beyond this bias, the current decreases, leading to a negative differential resistance in the IV curve. This negative resistance is exploited to de-attenuate the resonator formed by the diode's capacitance and the chip-integrated antenna's inductance, allowing for oscillations in the THz regime. RTDs therefore form an ultra-compact oscillator with minimal device count, high energy efficiency, and good impedance matching.

C. RESONANT TUNNELING DIODE DETECTORS

RTD structures may also be employed as sensitive THz detectors owing to their small capacitance and high nonlinearity at zero bias. Insertion of a third barrier, which results in a Triple Barrier Resonant Tunneling Diode (TBRTD) [24], leads to an asymmetrical current-voltage characteristic at zero bias which allows rectification. The high responsivity of a TBRTD detector integrated with a resonant slot antenna [25] was reported. Additionally, the wideband operation can be achieved by the integration of a TBRTD with a bow-tie antenna structure [26]. The highest averaged measured responsivity R_V was reported 900 V/W with the lowest computed NEP of 2.5 pW/$\sqrt{\text{Hz}}$ at 257.5 GHz when evaluated at zero bias [27], which would enable water content measurement in plant leaves in proximity of the specimen, when combined with RTD sources which exhibit output power of about 10 μW in this frequency range. The use of RTD structures for both transmitting and receiving THz signals holds promise for the realization of compact, low-cost, robust, and power-efficient THz transceivers, which can be applied in biological and agricultural settings.

D. PLANT LEAF WATER MONITORING USING A THZ RTD DETECTOR

Water is central to the functioning of a number of cellular processes. At a moderate water deprivation of short duration, the functions of cells are temporally impeded and can recover and restore all functions upon rehydration. Prolonged water deprivation will lead to irreversible cell damage and death. Air pollution, herbicide, etc., can cause some damage to the plant. A stressed plant leaf will exhibit a change in water content distribution. Thus, the plant water content and water transport dynamics can be assessed as a marker for health [28]. THz radiation has emerged as a promising non-destructive technique to study water content in plant tissues, allowing real-time monitoring of changes in water content under various stimuli indoor [29] and outdoor [30]. Traditional methods used to measure water content in plant tissues often require destructive techniques that damage or separate the organs of interest from the plant, making it difficult to monitor real-time changes. When a detached leaf dries out, its relative water content reduces at an exponential rate, and its thickness changes. This drying process can be conveniently monitored by performing transmission experiments using THz waves. In the THz region, since the absorption into water is large and the influence of water dispersion into biological tissue is small for long wavelengths, we can obtain transmitted images such as those of a plant leaf non-destructively based on information on moisture content [28]. Several works have been done for the detection of water content and water dynamics in different plant tissues under various conditions [31]. Most of them were based on THz-TDs systems which are bulky and expensive.

E. MEASUREMENT SETUP AND RESULTS

The THz water content measurements described here were done in the Integrated Systems Laboratory (headed by Prof. N. Pohl) at Ruhr University Bochum (Germany). The experimental setup, shown in Fig. 2(a), is composed of a THz wave generator (Keysight PNA-X vector network analyzer), a frequency extender module (VDI WR2.2 VNA-X), the RTD detector, a lock-in amplifier (MLFI from Zurich Instruments), a chopper wheel, and a PC for data acquisition. A horn antenna is connected to the waveguide output of the frequency extender. The THz wave, which is transmitted to the sample, is detected by the RTD detector, which can be operated at room temperature.

Fig. 2(b), which is the image of the receiver of Fig. 2(a), and (c) shows our own designed and fabricated single RTD detector chip integrated on the PCB test board and the E-beam fabricated logarithmic spiral antenna, respectively. The reduction in size and weight of several magnitudes between the conventional transmitter and the integrated RTD receiver is clearly visible from Fig. 2(a) and (b). The signal is read by the lock-in amplifier from the detector at 0.5 kHz chopping frequency and is fed into the PC. The signal frequency is swept in CW mode between 330 GHz and 500 GHz. A Geranium leaf is selected for the measurements. The sample (*cf.* Fig. 2(d)) is mounted on a perfect absorber to avoid standing waves and reflections from other parts of the measurement setup. The sample was placed in the middle between the frequency extender and the RTD detector; each was distanced 18.25 cm from the leaf.

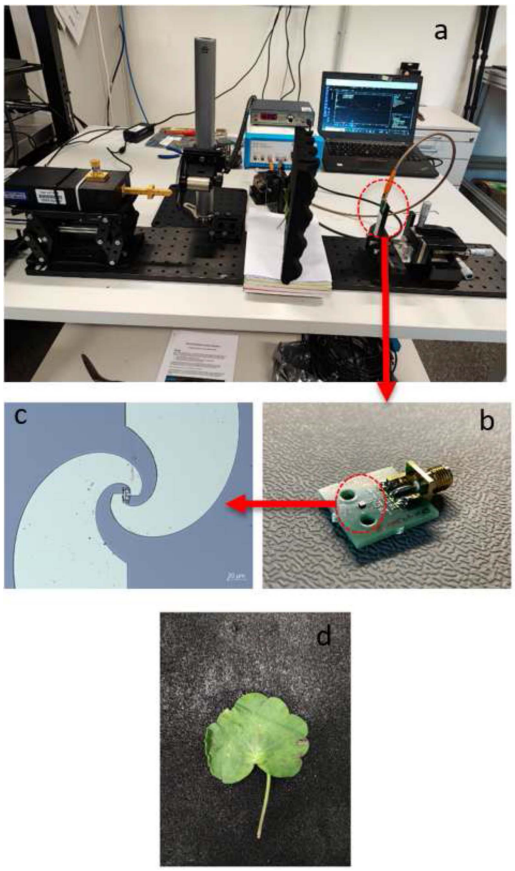

FIGURE 2. (a) The measurement Setup for the plant water monitoring with WR2.2 VNA-X from Virginia Diodes (VDI) and RTD detector module. (b) Single RTD detector chip integrated on PCB test board, used on the receive side of the experiment. (c) E-beam fabricated logarithmic spiral antenna. The TB-RTD is integrated between the two antenna arms. (d) The Geranium leaf, which is used as a sample for the measurements.

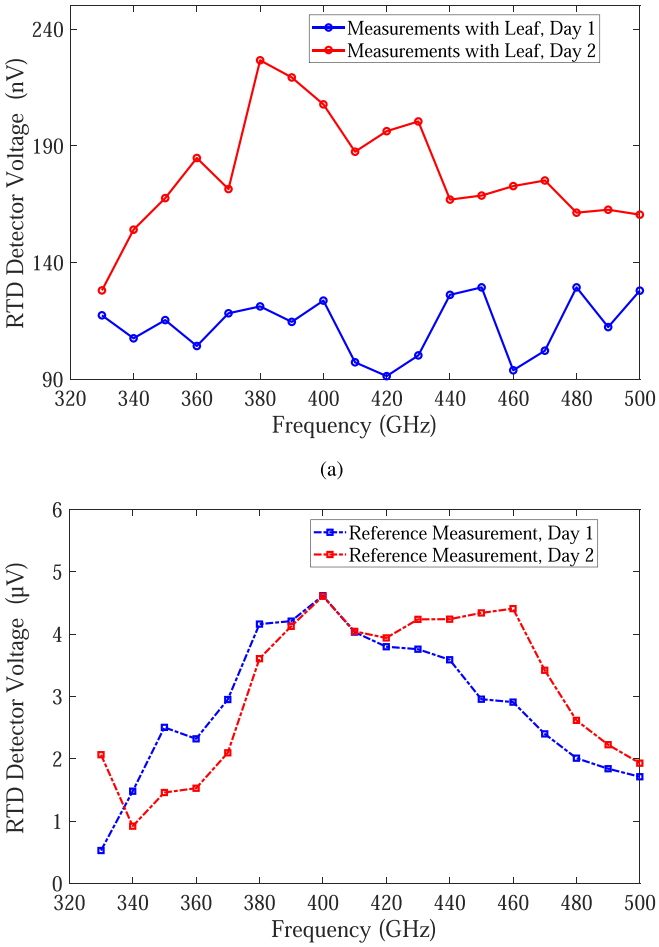

FIGURE 3. (a) The voltage recorded from the RTD detector during two consecutive days of measurements of a Geranium leaf. (b) The voltage was recorded from the RTD detector during two consecutive days of measurements without leaf (reference measurements).

In order to monitor the water content in the plant leaf, measurements were taken on the two following days. The voltage of the RTD detector was measured, which correlates to the water content of the sample, and also the weight of the leaf each day was measured using an electronic balance (FS-120 WAAGENET). Between the measurements, the leaf was kept for about 24 hours at room temperature. The temperature and humidity of the laboratory were in the range of 22.1−22.6 °C and 39.2−50.4%, continuously monitored by an environmental data logger (Testo). To evaluate the feasibility of the analytical method, we compared the measured, detected voltage of the RTD detector and the weight of the plant leaf. Due to the water loss of the leaf, THz absorption was reduced, and the voltage at the RTD detector at each frequency was increased, which can be observed in the plots of Fig. 3(a).

Additionally, for the reference measurements, the RTD detector voltage at each frequency was recorded by removing the Geranium leaf from the setup, which the recorded data are shown in Fig. 3(b). As can be seen from Fig. 3(a), there is a significant difference between the recorded voltage during the measurement days with the leaf; 5.2 dB increase in RTD detector voltage on the second day in comparison to the first day of measurements. However, in reference measurements without the leaf, Fig. 3(b), there is a negligible discrepancy in average recorded voltages as expected; 0.65 dB change. In parallel, we measured the weight loss of the Geranium leaf on the second day by electronic balance. Fig. 4 shows quantitatively the correlation of the THz detected voltage versus the leaf weight during the two days of measurements.

F. THZ-BASED IOT WIRELESS NETWORKS FOR IN-FIELD PLANT MONITORING

As a possible application use case for THz-based non-invasive, persistent plant monitoring, precision agriculture, or smart farming, is an emerging concept aimed at achieving resource conservation and crop yield optimization through a smart management system based on distributed plant monitoring [32], [33]. One envisioned approach is the aggregation of terahertz-based sensing data in a low-power, low-data-rate

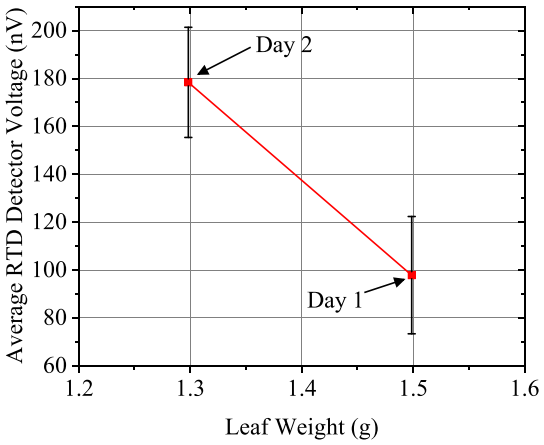

FIGURE 4. Representation of the correlation between the detected voltage from the RTD detector and the leaf weight (i.e. leaf mass) during the measurements with electronic balance, WAAGENET. The error bars indicate the variation from the average detected voltage in the whole frequency range of measurements (330−500 GHz).

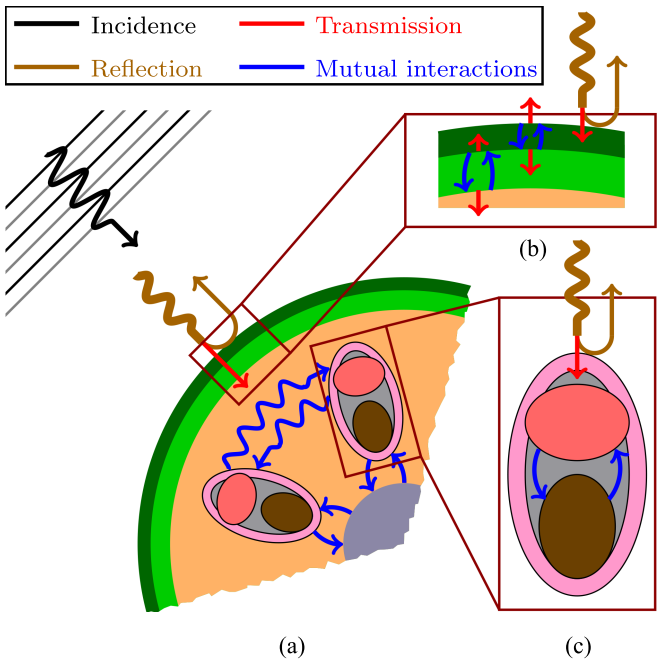

FIGURE 5. Schematic representation of a plant's stem including a selection of involved relevant electromagnetic interactions in the case of an illumination with a plane wave indicated by the arrows. (a) shows the overall cross section, (b) the layered interface of the stem's hull with the epidermis (dark green) and collenchyma (light green) separating the parenchyma (orange) from the surrounding medium, and (c) is a magnification of a vascular bundle, in particular the xylem (brown) and the phloem (light red), which are the channels carrying the water and electrolyte flows.

cellular wireless network to estimate plant health, in order to make intelligent farming decisions (fertilizing, watering, also on with localized control). For such systems, low-cost THz water content sensors based on robust electronic RTD transceivers which have both RTD oscillator and detector in a miniaturized module, could play an important role.

III. PLANT STEM IMAGING BY COMBINING RCS-MEASUREMENT AND SEMI-ANALYTICAL T-MATRIX BASED FIELD CALCULATION

Benedikt Sievert, Marvin Degen, Fabian Brix, Ute Krämer, Daniel Erni, Andreas Rennings

The non-invasive imaging of plants, for example the measurement of transport phenomena within them enables desired insights. This information can be used to draw conclusions about the metabolism of the plant [34], [35], resource allocation within the plant, and the impact of environmental factors [36]. Thus, we aim for a mobile THz sensor array that can be attached around the plant's stem to monitor long distance transport phenomena involving water, sugars [34], [35] and potentially other solutes, for example heavy metals [36], in a non-destructive manner. Before this ultimate sensor array solution, which can be applied in the natural habitats and in agricultural fields, we simple rotate the plant around the stem axis in front of a sub-THz radiator, measure the reflected signal and determine the radar cross-section (RCS) as a function of the turning angle. The second, equally important pillar of our imaging concept is the semi-analytical T-matrix-based field calculation [37], [38], [39], which is utilized here to guess the morphology and material parameters of the plant's stem based on the RCS agreement between measurement and simulation.

The efficiency of the simulation technique is due to a tailoring to the quite simple 2D topology of the plant's stem, which is visualized in Fig. 5. Inside a layer-wise homogeneous host-cylinder we have an internal structure including two types of vascular tissues, namely xylem and phloem [34], [35]. They differ in function and structure. The xylem is lignified. The basic function of the xylem is to transport water and nutrients from the roots to the shoots. The phloem, on the other hand, is made up of living cells and transports organic substances downwards inside the stem [34], [35]. Overall, this topology is ideally suited to be simulated using the T-matrix approach. Especially, for a large number of inclusions in the host cylinder, our tailored Recursive Aggregated Centered T-matrix Algorithm or short RACTMA [38] provides a high computational efficiency to solve the forward scattering problem and thus may play a key role in the inverse scattering analysis. With the use of the RACTMA we can precisely predict the EM field behavior in a full-wave manner outside the stem including the mutual interactions between the inclusions as well as the different layers of the stem, as visualized in Fig. 5.

The usage of our proposed RACTMA in this context is manifold. First, we can optimize our measurement setup based on the insights we got from simulation, which will be especially helpful for the more complex active THz near-field array concept, we aim for in the future. Second, we can correlate measurement data with simulation results, and enable prediction of the stem's inner structure by inversely fitting the simulation to the measurement in a very efficient manner.

In the following, we present the first steps towards the above-mentioned vision concerning 24/7 plant monitoring

with a mobile THz sensor in a natural population in the field. These steps include, firstly, a brief discussion of the T-matrix approach tailored to the special stem's cross-sectional structure, and secondly, a presentation of RCS measurement results of a plant stem mock-up. Here we show that the inverse fitting of the simulation results to the measurement works for the 3D-printed plant stem mockup. Finally, we quickly present a cylindrical position system, which is currently being built, and which is perfectly suited for the challenging imaging task, since the probes can be moved around the stem's surface in a precise manner. Additionally, we can switch to more advanced setups, like bi-static RCS measurements, offering more degrees of freedom (*cf.* Fig. 8).

A. T-MATRIX BASED CALCULATION OF EM FIELD SCATTERED BY THE PLANT'S STEM

We assume an invariance along the stem's axis yielding a 2D boundary value problem. The foundation of the T-matrix approach is the expansion of the unknown field quantity into a complete set of orthogonal basis functions, which are a solution of the wave equation. In the 2D cylindrical coordinate system case, the set of used basis functions are standing or outgoing cylindrical harmonics depending on the considered sub-domains.

Initially, each scattering element is analyzed in an isolated manner, by placing it into the locally surrounding medium as a host. The T-matrices relating the amplitudes of the incidence field to the scattered and transmitted field in both regions (inside and outside the scattering element) can be determined by integrating over the scatterer's surface using the extended boundary condition method (EBCM) [37]. For a circular scattering element, the integration can be done analytically, and the obtained matrices are diagonal. For all scattering elements without any inclusions, only the T-matrix relating the amplitudes of the regular background field to the amplitudes of the scattered field in the exterior is required in the following steps. For the other scatter (hosts with inclusions), a T-matrix of an equivalent scatterer having the same scattering characteristic as the union of all inclusions, including mutual interactions, embedded in an infinite domain with the same material properties as the host, is calculated by assuming the scattered field of each inclusion, besides the external field, as part of the exciting background field. This is done under application of translation matrices based on the Graf's addition theorems [40] and results in a linear system of equations to be solved for. In particular for a huge number of scattering elements, this system of equations may be hard to solve due to a) an increasing number of unknowns an b) its ill-conditioned nature. To circumvent this issue, recursive algorithms, like our tailored RACTMA [38] can be applied with a very high computational efficiency and numerical stability.

In a last step, the mutual interactions of the nested elements are considered again by enforcing continuity of the tangential field components under application of the matrices for the reflection and transmission determined in the first step. The finally obtained global T-matrix of the entire stem structure is independent of the incident field, and thus, can be used for the scattering analysis of arbitrary incidence fields (caused by aperture antennas, near-field probes etc.) coming from different angles by a simple matrix multiplication of the mentioned T-matrix with the amplitude vector of the incidence excitation field.

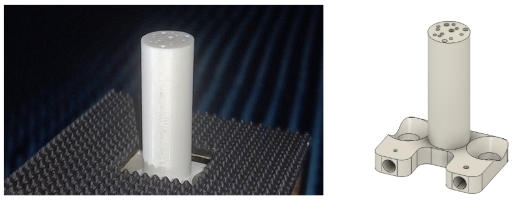

FIGURE 6. Photograph and CAD model of the 3D-printed plant stem mockup including several air-filled channels.

B. RCS MEASUREMENT OF MOCK-UP STEM STRUCTURE

Before the challenging imaging of a real plant, we consider a 3D-printed mock-up of a plant stem. This approach has several advantages, namely the geometry and material parameters of the structure are known a priori within certain limits. Therefore, either the measurement setup can be calibrated for best agreement with simulation, or the simulation parameters can be finetuned for an acceptable match with the measurement.

The mockup is 3D-printed using conventional white PLA with an outer stem diameter of 12 mm and an overall height of 40 mm (*cf.* Fig. 6). The model features 4 thick (diameter 1.5 mm) and 9 thin (diameter 1 mm) tubes. Both groups (thin &*amp*; thick) can be filled independently with fluids using e.g. demineralized or mineralized water. The PLA is modeled using a relative permittivity of 2.75 and a loss tangent of 2.5e-2, which also incorporates equivalent losses due to surface roughness of the 3D-printing process.

The simplest imaging setup for the stem mock-up is a reflection measurement carried out in the far-field. Here, only one horn antenna directly connected to a WR6.5 frequency extender (TxRx version operating from 110 GHz to 170 GHz) and a step motor that turns the stem mock-up is necessary. A monostatic RCS measurement for 120 GHz and 160 GHz is carried out. The corresponding results together with the semi-analytical simulation data are plotted in Fig. 3. In between the two polar plots the cross section of the plant stem mockup with air-filled channels of different diameters is shown (*cf.* Fig. 7).

By optimization of the essential stem's parameters, i.e., its material properties and allowing for small geometrical variations to account for manufacturing tolerances, the simulated data can be fitted nicely to the measured RCS. Given the large electrical size of the stem, the sensitivity to small geometrical variations and the relative permittivity of the mockup is high. This is challenging, as the parameter search of the inverse problem needs to be quite "global", of course within reasonable ranges. However, due to the very efficient

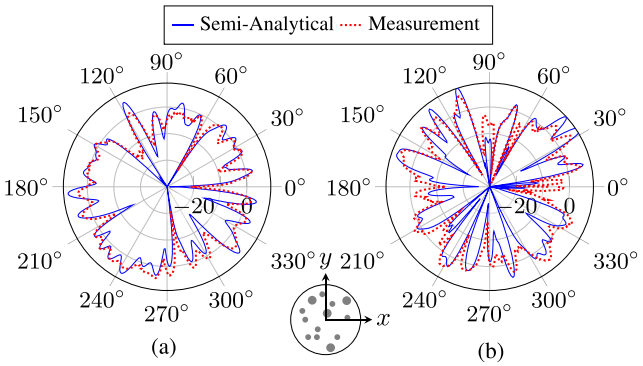

FIGURE 7. Normalized RCS calculated by RACTMA and measured at 120 GHz and 160 GHz as a function of azimuth angle. The agreement is, given the complexity of the model, and the significant sensitivity to material parameters and losses, very good, and has been achieved by fitting the model's material properties and mechanical uncertainties. Both RCS plots are normalized to give equal radiated power.

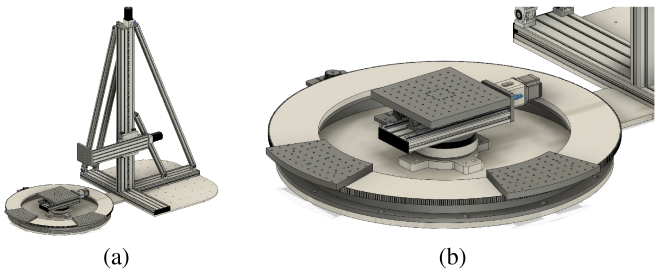

FIGURE 8. Future cylindrical positioning system offering extended scanning capabilities including bi-static RCS and along-the-stem axis measurements.

simulation scheme, we were able to find the geometric and material settings for an excellent RCS agreement.

Especially for the imaging of real plant stems, the solution to the inverse problem will be a lot more challenging since less a priori knowledge is available. Therefore, we are currently constructing a cylindrical positioning system (*cf.* Fig. 8) tailored to our imaging problem and offering extended options compared to the simple 1D RCS investigation we presented here. Besides a bi-static RCS investigation, we plan a mixed, maybe nested near- and far-field measurement series for accurate and reliable imaging of the plant. Additionally to EM field scanning in a transversal plane, measurements along the stem axis will be carried out for the hopefully successful investigation of fluxes trough the stem.

IV. THZ IMAGING OF LEAF AND INSECTS WITH VNA-BASED SETUP

Aman Batra, Fabian Brix, Fawad Sheikh, Andreas Prokscha, Ute Krämer, Thomas Kaiser

In this section, a vector network analyzer (VNA) based testbed is employed in a monostatic configuration to generate a high-resolution 3D image of leaves and insects using the SAR technique [41]. The images are evaluated further in accordance with the estimation of the link budget and surface properties, which is of significant interest to distinguish between an infested (termed as infected) and an uninfested healthy leaf.

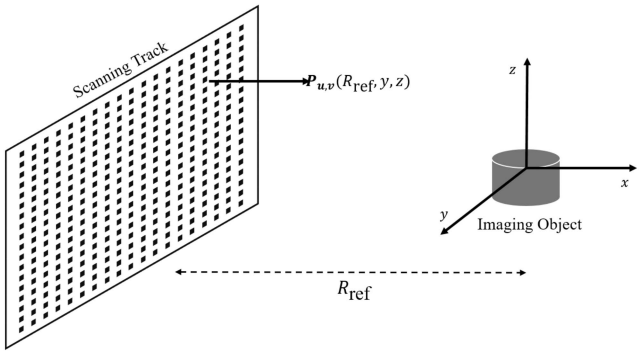

FIGURE 9. 3D SAR imaging geometry.

A. TESTBED

The experimental setup is composed of a VNA coupled to a frequency extender via cables. The low-frequency signal from the VNA is up-converted by the frequency extender into the desired spectrum of 330–500 GHz. A horn antenna of length 1.93 mm and a gain of ∼25 dB is mounted on an extender waveguide flange. With this configuration, a range resolution proportional to bandwidth corresponds to 0.88 mm, and an angular resolution of ∼1 mm is achievable [41]. To form the SAR trajectory, the frequency extender is mounted on a motorized Y+Z stage. The SAR imaging geometry of 3D image acquisition of an object located at reference distance R_{ref} is shown in Fig. 9. The range direction is along the x-axis and y- and z-axis represent the azimuth and elevation directions, respectively. In the monostatic configuration, the transceiver or the extender in the current setup located at $P_{\text{u,v}}$ follows a trajectory along y- and z-axis, and a 2D scanning track is obtained. The aperture positions in the track along azimuth and elevation directions are represented by $u \in (u_1, N_U)$ and $v \in (v_1, N_V)$, where N_U and N_V are the numbers of positions along y- and z-axis, respectively. In this work, the trajectory is implemented with $N_U = 161$ and $N_V = 151$ with a step-size of $\delta u = \delta v = 1$ mm. At each aperture position, S11 reflection coefficients are captured with 3001 frequency points and $R_{\text{ref}} \approx 37$ cm.

For image reconstruction, the gathered raw data is processed with the time-domain Back-Projection Algorithm (BPA). The detailed description of the testbed components/devices and BPA is available in [41]. Furthermore, two imaging environments are considered. The first environment is defined as A, which focuses on plant monitoring where two leaf samples of the plant Geranium are considered as shown in Fig. 10(a). One of the leaves shown in Fig. 10(a) belongs to a plant that is infested with aphids, which are sap-sucking insects. With time, the aphids grow and leave their skin on the leaf surface as visible in Fig. 10(a). The leaf of an uninfested plant, which is marked in Fig. 10(a).

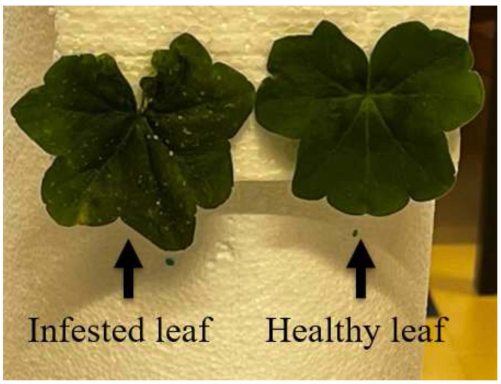

(a)

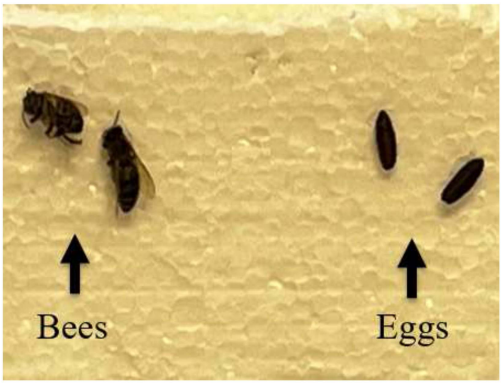

(b)

FIGURE 10. Imaging environments with (a) infested (termed as infected) and uninfested healthy leaf and (b) insects.

The second environment addresses insect monitoring and is termed here as environment B. The environment consists of honeybees and eggs of blow flies which belong to the family of *Calliphoridae*. The photo of the mapping environment is shown in Fig. 10(b). The orientation of the bee is important in defining the scattered power from the bee's front and back surfaces. Therefore, two bees in a different orientation as shown in Fig. 10(b) are pasted on a styrofoam.

B. RESULTS

With the presented testbed in Section II.A, the raw data is captured and processed with BPA for 3D image reconstruction. The resulting 3D images and evaluated properties for both environments are presented in this section.

In Fig. 11, the resulting SAR image of the environment A is shown. Focusing on the leaf surface, the resulting image based on maximum intensity projection (MIP) scheme [42] along range direction is presented. A high-resolution image of the leaves is obtained and the intensity scale is normalized with respect to the maximum magnitude of reflection from the mapped environment, which is provided by the healthy leaf in the range of −72 dB. For the infested leaf, the complete leaf surface is observable. However, the skeleton of a healthy leaf is not flat compared to the infested leaf. The curved side portion of the healthy leaf resulted in weak reflection. It is

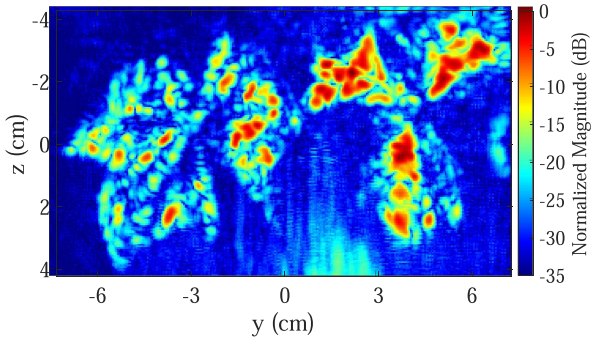

FIGURE 11. SAR image of environment with infested and uninfested (healthy) leaf.

assumed that the energy received from the curved portion is below the noise level of the employed system. Hence, the curved portion is not visible in the resulting SAR image. For evaluation of the differentiation between the leaves, the mapped leaf area in the second quadrant is considered and shown in Fig. 12, where Fig. 12(a) and (b) represents the area from the aphid-infested and the healthy leaf, respectively. Considering the surface scattering mechanism, there can be two primary sources of differentiation. First is the reflected power from the leaf. The healthy leaf surface is smoother in comparison to the infested leaf. Besides, the presence of leftover remains of the aphids also increases the roughness. With the employed SAR geometry, the smoother surface results in higher reflected power, and the same is observed. From Fig. 12, it is estimated that the maximum magnitude of reflection from the infested leaf is around ∼6 dB lower than the healthy leaf. Second is the formation of the leaf surface. It is observed that the mapped area of the leaf surface of the infested leaf has a larger degree of discontinuity in comparison to the uninfested control, as visible in Fig. 12(a) and (b). One of the causes for this could be the disruption in surface properties of the infested leaf resulting from the presence of aphid remains and an unbalanced distribution of water.

Similar to the environment A, a high-resolution image of mapped space with insects is acquired and shown in Fig. 13. The outer shell of the honey bee reflects significant energy and hence the three main body parts of the bee anatomy, which are the head, thorax, and abdomen, are observed in the resulting SAR image shown in Fig. 13(a). As the bee's front- and back body are not symmetrical, it is examined that the reflected energy from the bee's back body is comparatively less than the front. It differs by a magnitude of around 10 dB. Furthermore, both the eggs of blue flies are also well mapped as shown in Fig. 13(b).

V. MILLIMETERWAVE RADAR IMAGING FOR INSECT MOTION SENSING

Ingrid Ullmann, Konstantin Root, Martin Vossiek

As a preliminary study, we conducted a scaled experiment for the envisaged system and application. Whereas the ultimate goal is to use THz radar for monitoring very small

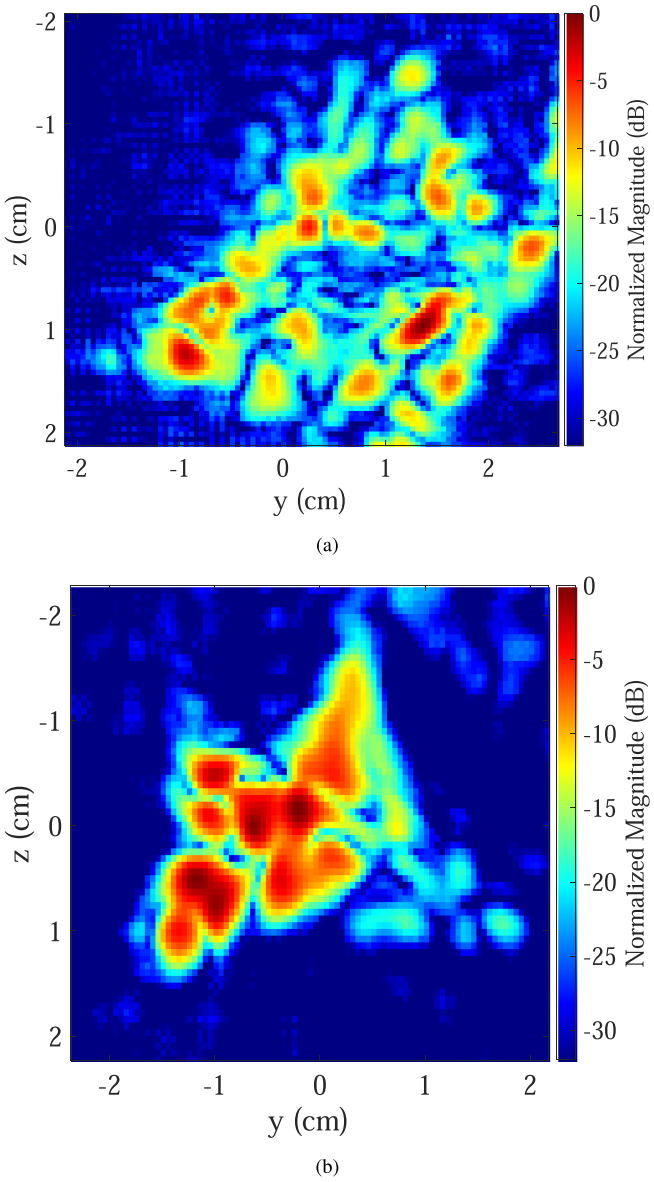

FIGURE 12. Mapped area for evaluation of differentiation between (a) an infested leaf and (b) an uninfested (healthy) leaf.

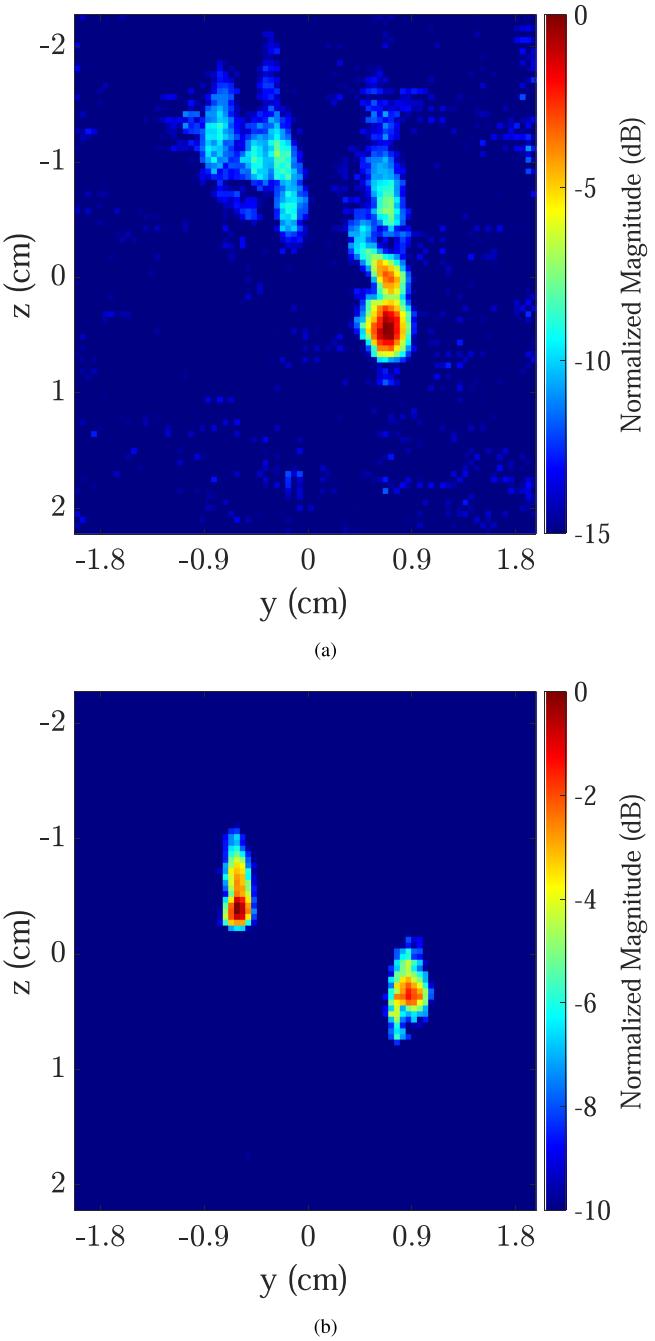

FIGURE 13. SAR image of environment with insects, (a) honey bees and (b) eggs of blow flies.

insects such as aphids, in the preliminary study, a millimeter-wave radar that is already available was used. Since with such a radar it seems impossible to monitor insects of the size of an aphid, we imaged insects of larger size. The results are expected to translate to smaller sizes of insects for shorter wavelengths (i.e. higher frequencies in the THz range).

For the preliminary study, we measured the movements of a ladybug (*Coccinellidae*), which had a length of approximately 8 mm. We used a multiple-input-multiple-output (MIMO) imaging radar, operating in stepped-frequency-continuous-wave mode at 72 GHz–82 GHz. The MIMO radar has 94 transmit and 94 receive channels. It allows for a range resolution of approx. 15 mm and a lateral resolution of approx. 3 mm at a distance of 20 cm. In the experiment, the insect was placed on a plant located at approx. 18 cm in front of the radar. The plant was tilted so that its leaves faced the radar, as shown in Fig. 14.

A sequence of radar data was recorded while the insect was moving freely on the leaf. For each time frame, an image was reconstructed. Each image shows the reflection from the leaf and that from the insect, as shown in Fig. 15(b). As can be seen, compared to the photo on the top, it is hard to recognize the bug. To display the bug's movement more clearly, it is useful to cancel out the leaf's reflection. In order to do so, we subtracted the average of the previous 10 frames from

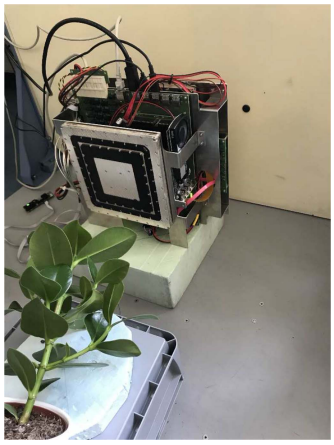

FIGURE 14. Measurement setup consisting of millimeter wave MIMO imaging radar and the plant onto which the insect was placed.

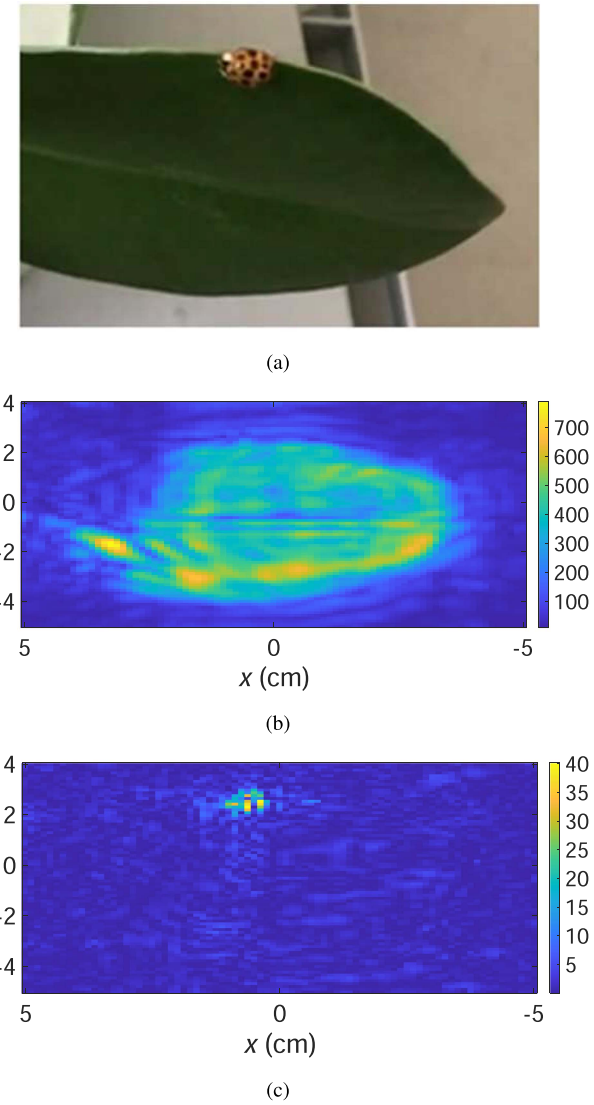

FIGURE 15. (a) Ladybug on the leaf, (b) reconstructed radar image, and (c) image with compensation of leaf.

each image. It is assumed that the leaf's reflection does not change over this time, whereas the location of the insect's reflection changes as it moves. A subtraction image is shown in Fig. 15(c) on the bottom. A reflection, which corresponds to the insect, is now clearly visible.

Fig. 16 shows a number of frames from the recorded sequence of reconstruction images. A sequence of photos is shown in Fig. 17. The camera was not time-synchronized with the radar. The trajectory on which the insect had been moving can be reconstructed from the radar images. It is shown in Fig. 18, along with the reflection of the leaf. The trajectory is reasonable when comparing it to the photos.

VI. EXPERIMENTAL RCS DETERMINATION AND IMAGING OF HONEY BEES WITH THZ TIME-DOMAIN SPECTROSCOPY

Tobias Kubiczek, Jan C. Balzer

The RCS describes how much energy is reflected from an object under a certain angle. The relationship between the wavelength (= frequency) of the electromagnetic wave and the object size plays a central role. If the wavelength is much smaller than the object, the wave is reflected from the surface. If the object size is much smaller than the wavelength of the electromagnetic wave, the object may be invisible to the radar. Currently, radar systems with a frequency in the range of 6 GHz to 12 GHz are commonly used for the RCS determination of insects [43], [44]. Recently, investigations have been carried out to measure the activities of honey bees at 24 GHz [15] and 77 GHz [45]. Here, the wavelength is in the order of insects. Thus, no details can be detected. Therefore, it is imperative to move to higher frequencies to reliably detect and classify smaller insects. In the following, we will show the first RCS measurements on bees beyond 300 GHz.

For the broadband RCS measurement, a THz time-domain spectroscopy (THz-TDS) system is employed. A sub-100 fs laser pulse from a mode-locked fiber laser is down converted into the THz frequency range via a photoconductive switch. For the detection, a similar device is used. The conductivity is gated by the same laser pulse, while the photocurrent is measured. The photocurrent is proportional to the incident THz wave. The temporal resolution is achieved by delaying the laser pulse at the detector. In this way, electromagnetic waves with frequencies between 100 GHz and 6 THz can be generated and detected. A detailed overview is given by Balzer et al. [46].

To measure the RCS of a honey bee, a bistatic setup is chosen since no optoelectronic transceivers for a monostatic setup are commercially available. An overview of the setup is shown in Fig. 19. The divergent beam from the transmitter antenna (Tx) is collimated by a low-loss TPX lens with a focal length of 50 mm. Within the collimated radiation, a honey bee with a sample holder is attached to a turntable to enable angle-dependent RCS measurement. The scattered electromagnetic wave is detected by the receiver antenna (Rx). The

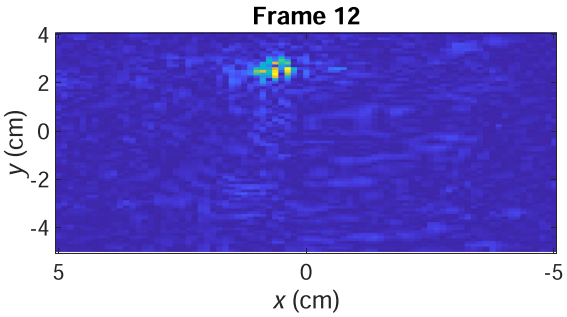

(a)

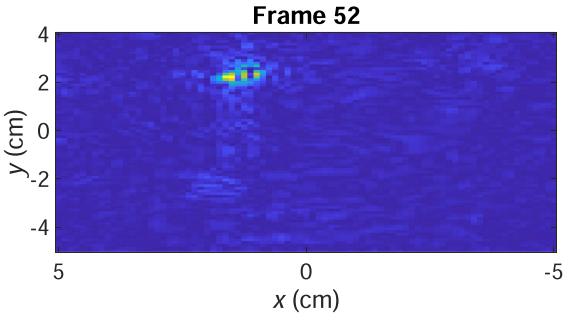

(b)

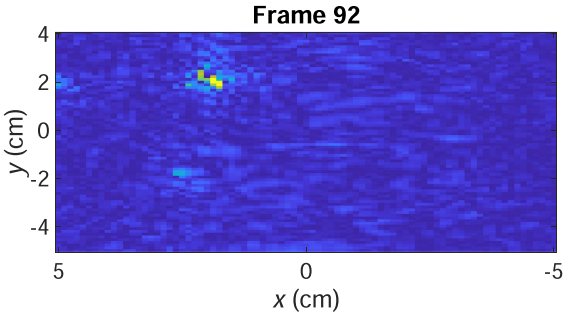

(c)

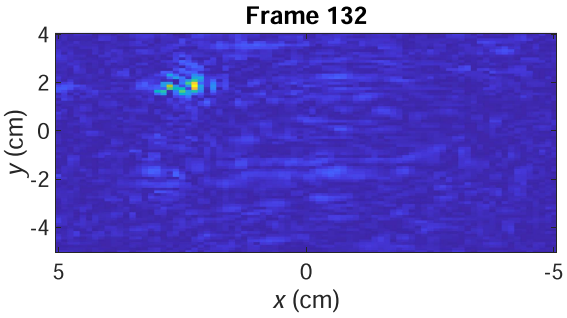

(d)

FIGURE 16. Sequence of radar image reconstruction frames.

(a)

(b)

(c)

(d)

FIGURE 17. Sequence of photos showing the bug's movement.

angle between Tx and Rx is 30°. Since the energy scattered by the bee is expected to be low, it is important to use a sample holder with a minimal RCS. Therefore, we designed a cone with a base diameter of 15 mm and an angle of 9° leading to a height of 50 mm. The side view of the sample holder is shown in Fig. 19(b). Assuming an ideal surface, the cone reflects the incident electromagnetic radiation away from the receiver. The sampler holder was fabricated by an Ultimaker S5 fused deposition modelling (FDM) 3D printer. Tough polylactid was used as the material.

The bee used for the study, was soaked in ethanol fresh after its natural death by a beekeeper. This is to prevent the bee from drying out to enable the most realistic measurements possible. The ethanol-soaked bee was then glued onto the sample holder. A photo is shown in Fig. 19 For the measurement, the

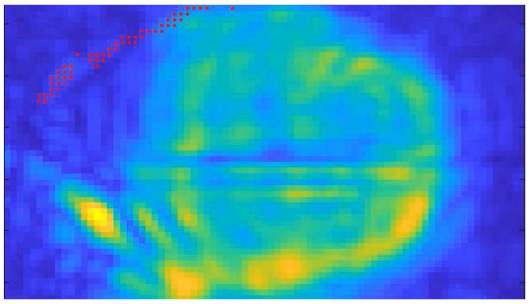

FIGURE 18. Radar image of the leaf and reconstructed trajectory of insect movement, indicated by red dots.

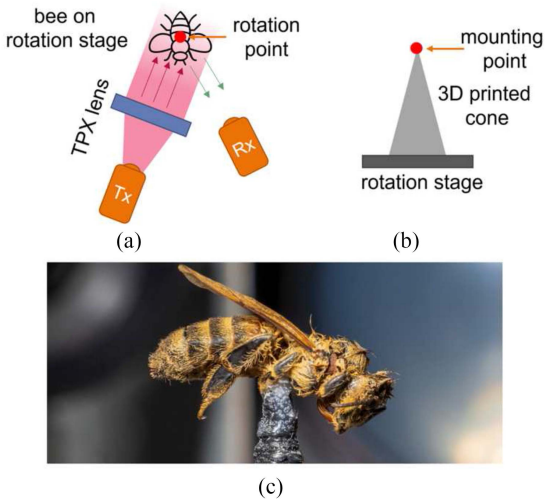

FIGURE 19. Measurement setup with (a) schematic of the top view. (b) schematic of the sample holder, and (c) a photograph of the mounted bee.

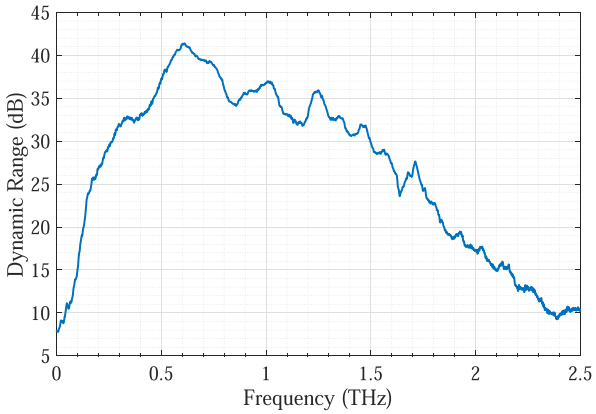

FIGURE 20. Dynamic range of the employed setup, calculated by substracting a measurement without any sample and a measurement without any sample and a measurement against a metal plate as a reference measurement.

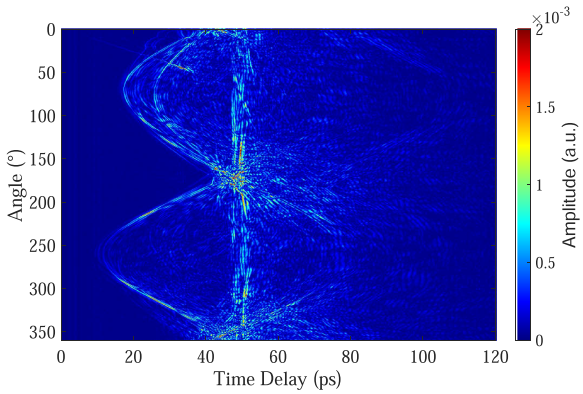

FIGURE 21. Radargram consisting of the recorded intensities for each step after band pass filtering and removing frequency components lower than 100 GHz and above 3 THz.

bee was rotated by 360° in 0.3° steps. At each position, the reflected radiation was measured, and 2000 THz-TDS traces were collected and averaged. In addition, an empty measurement without the sample holder and a reference measurement against a metal plate was performed. To investigate the limitations of the measurement setup, a dynamic range calculation was performed by subtracting the amplitude spectrum of the empty path from the amplitude spectrum of the reference measurement. The result is shown in Fig. 20. The dynamic range at 150 GHz is 24 dB and increases for 250 GHz to 30 dB. The peak dynamic range is reached at 605 GHz with 41 dB. This dynamic range allows the determination of the RCS in the range from about 100 GHz up to 2 THz.

First, in Fig. 21(a) diagram of the recorded intensities for all angular steps as a function of time, also called *radargram*, is shown. The delay range of 50 ps is dominated by reflections from the sample holder. Here, it is noteworthy that this comes from the scattering of the glue which is used to fixate the bee. The other reflections can be attributed to the bee. This demonstrates that the setup is capable of detecting reflections from a bee with a high resolution. To further ensure a proper calculation and enhance the quality of the calculated RCS, a windowing of the radargram must occur to remove the reflections of the sample holder. Here an inverse Tukey window was used with a 10 ps width centered around the time delay of 49 ps. In addition, broadband Tukey windowing is performed over the entire time trace to smooth the edges and ensure a correct fast Fourier transform (FFT) without discontinuities.

Fig. 22 visualizes the reflected intensity normalized by the reference measurement performed against a metal plate for 145 GHz, 244 GHz, 462 GHz, and 945 GHz. The head of the bee is oriented in the 0° direction, as indicated in the figure. Since the total power of the incoming wave cannot be measured in this measurement geometry, these representations do not correspond to the RCS, but to an equivalent representation.

At 145 GHz and 244 GHz, high reflectivity is seen from the side of the bee at 270°. In addition, other features are clearly visible at different angles that could be assigned to a wing, the head, and the feet of the bee. Since the resolution for detectable features also increases with higher frequencies, the plots for 462 GHz and 945 GHz show many narrow deflections. However, the complex surface structure of the

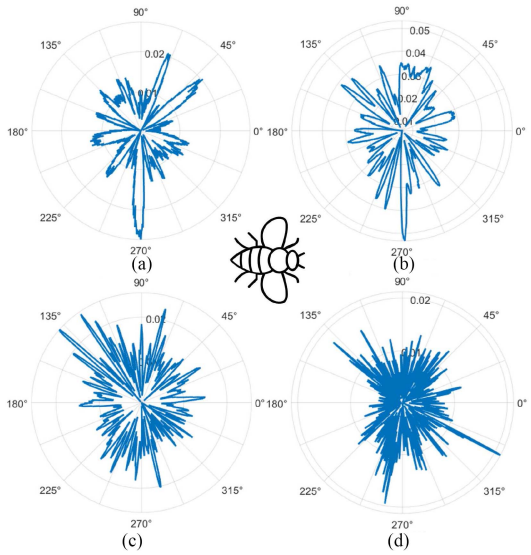

FIGURE 22. Measurement normalized reflection factor from a bee measured in bistatic geometry for different rotation angles and frequencies (a) 145 GHz, (b) 244 GHz, (c) 462 GHz, and (d) 945 GHz. The bee in the middle is indicating the orientation of the bee with respect to the plots. The head of the bee is orientated in 0° direction.

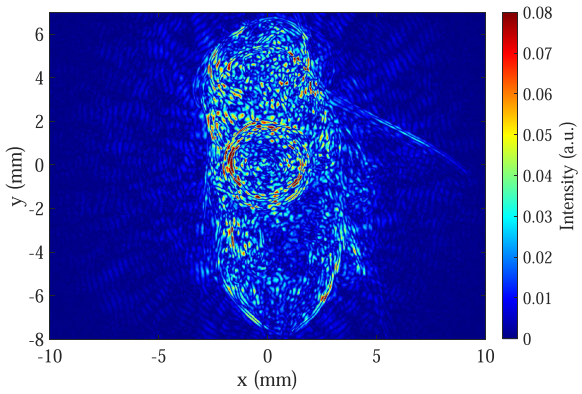

FIGURE 23. Back-projected measurement of rotated bee.

bee makes interpretation of the localized peaks difficult. To validate the measured RCS, we use a back-projection algorithm for a 2D reconstruction of the recorded data [47], [48]. This corresponds to the inverse synthetic aperture radar (ISAR) imaging [41]. As the incoming radiation is collimated, the presented algorithm was altered by changing the position of the transmitting antenna to a far distance to emulate the collimated beam. The result can be seen in Fig. 23, revealing the body shape of the bee. In addition, the tip of the sample holder can be seen centered in the bee body and the right wing of the bee.

VII. TRACKING OF HONEY BEES INSIDE THE HIVE USING THZ HARMONIC RADAR

Kevin Kolpatzeck, Jan C. Balzer

Radar systems are a promising solution for tracking insects in their natural environment. Unlike cameras, they can operate in the dark and make it possible to follow an insect's movement even if it is concealed by plant parts. However, the small RCS of an insect makes it difficult to distinguish it from the highly scattering environment in which it often resides. A good solution to this problem is the use of harmonic radar. An antenna tag containing a non-linear device is placed on an individual insect, so that it re-radiates the second harmonic of the radar's transmit signal. A receiver that only receives the second harmonic blocks out the linear clutter of the environment and detects the tagged insect with high sensitivity. The potential of entomologic harmonic radar has been demonstrated in the microwave range up to about 20 GHz for the tracking of – among other insects – moths [49], honeybees [50], bumble bees [51], carabid beetles [52], butterflies [53], and hornets [54]. Distances of up to 1 km have been reported [55]. A comprehensive review of entomologic radar including a comparison to other methods for insect monitoring is given in [56].

There is great scientific interest in being able to track individual honeybees – specifically the queen bee – not only outdoors but also inside the hive. This is impossible with existing systems for two main reasons. Firstly, microwave radar with a wavelength of a few centimeters cannot provide the sub-cm accuracy required for tracking the motion of a bee across and between individual honeycombs. Secondly, the size of the antenna tag is determined by the frequency being used and is thus of the order of several millimeters. Such a large antenna does not allow the bee to move freely within the hive [55]. Both problems can be solved by moving into the THz frequency range.

A THz harmonic radar makes it possible to track insects with (sub-)millimeter accuracy. Moreover, small planar antennas for the THz frequency range can be easily placed on the opalite bee signing plate that is customarily used to mark the queen bee within the hive without hindering its natural movement. One challenge of using THz radiation within a beehive may be the reflection and absorption losses of the honeycombs. A photograph of a styrofoam bee mating box that can be conveniently used as a lab-sized beehive containing three honeycombs and a photograph of an individual honeycomb are shown in Figs. 24 and 25, respectively.

To quantify the transmission loss, we perform transmission measurements of different vacated honeycombs using a Menlo Systems Tera K15 THz time-domain spectroscopy (THz-TDS) system. The collimated THz beam that passes through the honeycomb has a diameter of approximately 15 mm. A photograph of the measurement setup and plots of the measured transfer functions are depicted in Figs. 26 and 27, respectively. The transfer functions show a strongly frequency-selective behavior that varies strongly among the three different samples. Most notably, there are strong resonances in the frequency range between 200 GHz and 700 GHz that can be attributed to multiple internal reflections within the honeycomb. The experiment showed a strong dependence of the resonant frequencies and the depth of the resonances on the angle of incidence. The attenuation in the frequency range

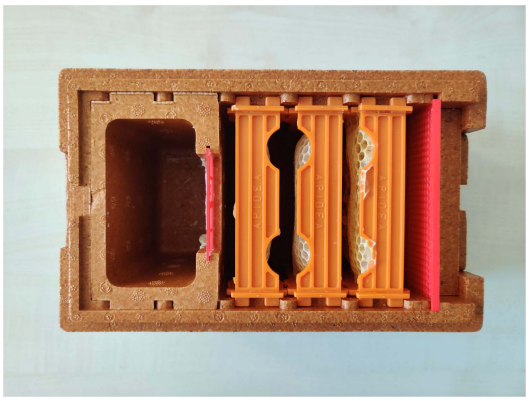

FIGURE 24. Styrofoam bee mating box containing three honeycombs.

FIGURE 25. Sample of a single vacated honeycomb.

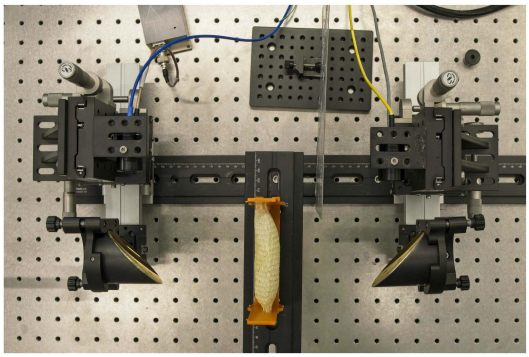

FIGURE 26. Photograph of the THz-TDS transmission setup for measuring the transfer functions of honeycombs.

above 700 GHz is strikingly flat with values ranging between −12 dB for honeycomb 2 and −26 dB for honeycomb 3. For tracking the queen bee within the hive using harmonic radar, the lower end of the THz range, particularly the frequency range below 200 GHz, appears to be a good candidate. It should be noted that the apparently strong frequency dependence visible in the plot for frequencies below 200 GHz can be attributed to the lacking dynamic range of the THz-TDS system at those frequencies.

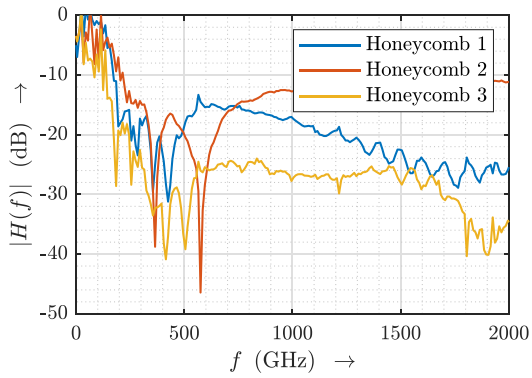

FIGURE 27. Measured transfer functions of three different vacated honeycombs.

VIII. THZ INTERACTION WITH WESTERN HONEY BEES

Mandana Jalali, Jan Taro Svejda, Daniel Erni

Insects are vital entities of our ecosystem, whose populations are dramatically diminished due to overuse of pesticides as well as the decline of available habitats. It has been recently conjectured in an evaluation report issued by the Swiss administration [57] that the progressing diffusion of 5G and future 6G mobile communication services into the living world and the ecosphere may affect arthropodes in a different way than postulated in the regulation framework for the electromagnetic (EM) exposure limits proposed by ICNIRP [58]. Because of their small size and the resulting conformity to operating wavelengths insects may suffer from an increased sensitivity against EM radiation in particular at frequencies in the multi-GHz up to the THz range. Given their vital role as pollinators, honey bees are of particular concern since the number of their colonies dropped by the turn of the millennium [59]. Although these figures are currently increasing, the 24/7 real-time monitoring of European honey bees *(Apis mellifera)* has revived the 70+ year tradition of radar entomology in remote sensing in ecology and conservation [56].

The main focus of radar entomology usually lies in (precision) migration path tracking, as well as mass, density, and number estimation of insect swarms. Our vision on honey bee monitoring addresses interactions in the close ecosphere around plants allowing for a 24/7 observation of e.g. the dynamical flight patterns and the duration of stay (on the blossom) using their highly specific mm-wave/THz RCS for identification and selection [60] against alternative pollinators (or pests). Such a modern approach would allow to track the kinetics of social behavior of honey bees in their habitats and natural environment in order to detect environmental stress, as well as understanding their complex dynamics. This may also include the observation of e.g. queen bee movements in bee hives as well as the assessment of the energy intake of honey bees when exposed to mm-wave up to THz radiation and its comparison to the ICNIRP safety limits [58]. In [61], [62], pioneering EM exposure studies were performed on western honey bees in the frequency range of 0.6−120 GHz, distinguishing between worker bees, drones,

TABLE 1 Experimental Data for the Effective Dielectric Function (i.e. The Permittivity and Conductivity) of Western Honey bees [62]

Frequency (GHz)	ε_r	σ (S/m)
0.6	45.6	0.688
1.2	44.2	0.924
2	39.9	1.35
3	38.8	2.05
6	38.0	5.05
12	28.6	12.0
24	14.9	21.1
60	7.018	27.9
120	5.46	29.2

larvae, and queens, and confirming an increased absorption when aiming at 5G frequencies (and beyond). In either case, namely in EM dosimetry [62] and RCS analysis [44] for radar-based bee monitoring, anatomically detailed full-wave computational EM models in conjunction with realistic experimental validation become increasingly important.

Accordingly, the interaction of EM radiation with a European honey bees is numerically investigated in the range of 10 GHz up to 500 GHz.

The study relies on a conformally accurate EM 3D model of the honey bee for either a virtual dosimetry or a scattering analysis. This digital twin is based on a realistic 3D image model with a shell mesh in STL format. The latter is imported into the FEM-based simulation platform COMSOL Multiphysics in order to fix and modify the mesh for a subsequent conversion into a volumetric object. COMSOL with its unstructured mesh is well suited for this task and simultaneously serves as a prime reference model for our digital twins.

The corresponding material properties of the honey bee's inner structure, namely its dispersive permittivities and conductivities are required. Currently, only few data on aggregate effective material parameters in the lower frequency ranges are available [62] (*cf.* Table 1).

Based on this data set a bulk material model for the honey bee has been set up where its frequency range is further extended into the THz range using a multipole Debye model [63] (*cf.* (1)) keeping the first four terms in the summation.

$$\varepsilon = \varepsilon_\infty + \sum_{i=1}^{4} \frac{\Delta\varepsilon_i}{1 + j\omega\tau_i} + \frac{\sigma_s}{j\omega\varepsilon_0} \tag{1}$$

The measured sparse data of Table 1 are first interpolated using corresponding spline functions, yielding an extended data set. This set is then used for the nonlinear function fitting of the Debye model, where 10 coefficients have to be determined within an evolutionary algorithm-based optimization procedure, which minimizes the least-square error between experimental data and Debye model. The resulting dielectric function covers now the whole frequency range of interests namely from 0.1 GHz up to 2 THz where its permittivity and conductivity are illustrated in the Fig. 28, while the fitted

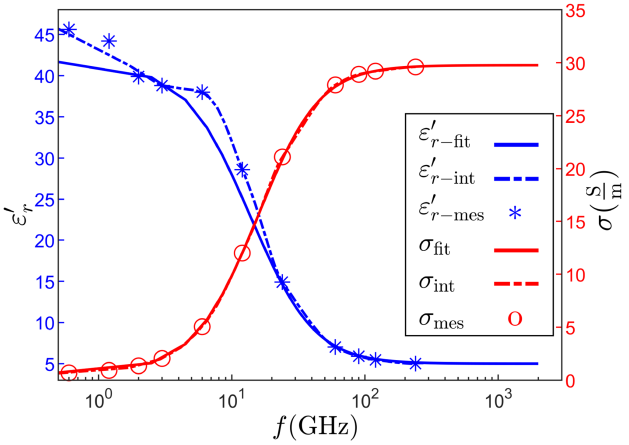

FIGURE 28. The retrieved dielectric function showing the Debye model of the permittivity (solid blue line), the interpolated measured permittivity (dash-dotted blue line), the Debye model of the conductivity (solid red line), and the interpolated measured conductivity (dash-dotted red line). The fitted conductivity is very close to the interpolated measured conductivity and hence the red dash-dotted line is hardly visible. The markers depict the available experimental data [62].

TABLE 2 The Coefficients of the Fitted Debye Model for the Four First Terms in the (1)

ε_∞	$\Delta\varepsilon_1$	$\Delta\varepsilon_2$	$\Delta\varepsilon_3$	$\Delta\varepsilon_4$
5.0	19.0	17,7	8.6	8.6
τ_1 (ps)	τ_2 (ps)	τ_3 (ps)	τ_4 (ps)	σ (S/m)
84.2	1854	16.8	16.8	0.6

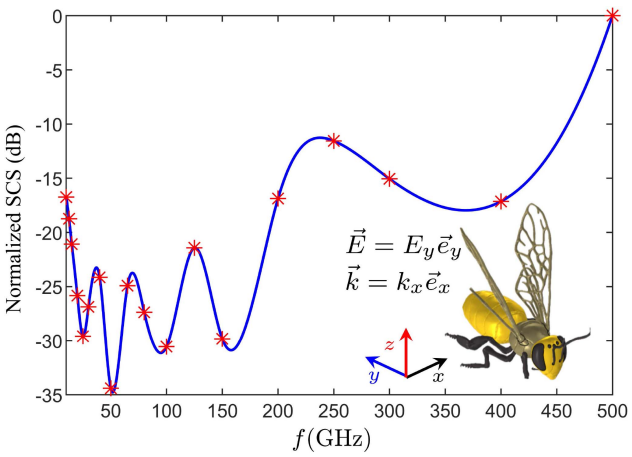

FIGURE 29. Simulated spectral response of the normalized SCS of the honey bee for a plane wave illumination from the left (i.e. x-direction). Typical RCS values are estimated between -38 dBsm and -43 dBsm at 40 GHz for y-polarization.

Debye coefficients are summarized in the Table 2. Currently we are focusing on the inner anatomy of the bee in order to complement the present bulk model with the cuticula and the most relevant organs.

For both, the exposure and scattering analysis, the volumetric bee model (*cf.* Fig. 29) together with the established

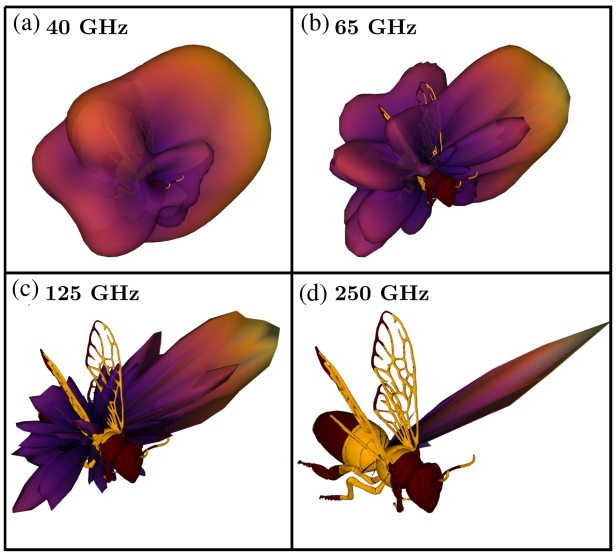

FIGURE 30. 3D-FDTD simulation of the far field scattering patterns of the European honey bee at (a) 40 GHz, (b) 65 GHz, (c) 125 GHz, and (d) 250 GHz.

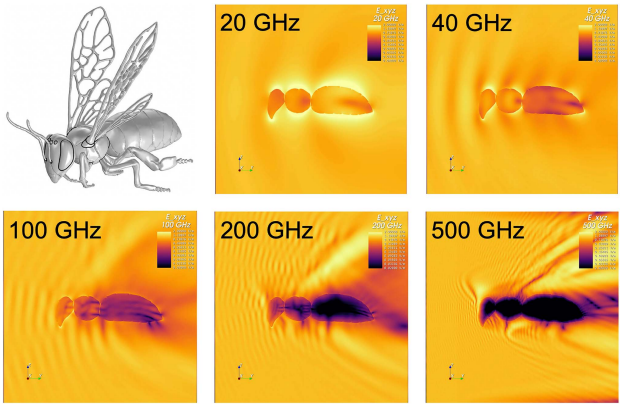

FIGURE 31. 3D-FDTD simulation of the electric field's absolute value for a plane wave illumination from the left (y-direction). The field distribution displays the penetration behavior into the volumetric bee model at different frequencies between 20–500 GHz.

Debye model are imported into the finite-difference time-domain (FDTD) computational electromagnetics simulation platform EMPIRE XPU. The bee model is illuminated with a plane wave from the left (x-direction) while covering the frequency range 10−500 GHz. The resulting spectral response of the normalized scattering cross-section (SCS), is depicted in Fig. 29.

The normalized SCS of the honey bee displays distinct peaks at 40 GHz, 65 GHz, 125 GHz, and 250 GHz, where the associated far field scattering characteristics are illustrated in Fig. 30. Such spectral fingerprints may become characteristic for the identification of honey bees in insect monitoring together with the azimuthally resolved RCS (not shown here) at a corresponding frequency.

A preliminary account towards a virtual dosimetry of the honey bee is given in Fig. 31 displaying the electric field penetration into the volumetric bee model. The light halo at 20 GHz hints towards a resonant interaction due to the commensurability between wavelength and bee size. At frequencies above 100 GHz the field, penetration gets less prominent and wings and legs start contributing to the scattering cross section.

A resilient virtual dosimetry has to rely on power densities in conjunction with specific absorption rates (i.e. SAR values) in the bee's proper inner anatomy. First steps towards an inhomogeneous bee model have already been taken by including the thin exoskeleton (cuticula) based on experimentally validated material properties. A brief numerical analysis has already shown that the shielding effect by the cuticula is rather small, which is, though, a surprising result.

IX. 3D PHOTOREALISTIC THZ RAY-TRACING SIMULATIONS FOR INSECT SENSING

Fawad Sheikh, Andreas Prokscha, Aman Batra, Dien Lessy, Baha Salah, Thomas Kaiser

Sensing the slow movement of a tiny object requires high frequency, which improves the ability to perceive subtle details and alterations in movement. The level of detail that can be acquired relies on the resolution, which is determined by the wavelength of the waves employed to sense the object. THz frequencies seem promising to provide sub-millimeter accuracy for sensing micro-motion in tiny objects.

Measuring living organisms, particularly small ones such as insects, can pose a significant challenge due to their size and mobility. However, a potential alternative solution is to conduct 3D Photorealistic THz Raytracer (PRT) simulation from TMTC [64] which can offer initial results for studying THz sensing with reduced computation time compared to full wave simulation. This PRT is capable of integrating a wide range of fascinating and intricate details of insects, ranging from the unique patterns on their wings and bodies to the fine structures of their legs and antennae. Therefore, these intricate structures can imitate the random roughness of insects, which is significant in the context of THz frequencies.

A. MICRO-MOTION SIGNATURES FROM VARROA MITE

Varroa mites (*Varroa destructor*) are external parasitic mites that infest honey bees [65], [66]. The body of Varroa mites is covered with a layer of hair-like projections, known as *setae*, which give them a rough appearance. The *setae* are thought to be important for the mites' ability to cling onto the bees and move around their body. If left unchecked, Varroa mites can lead to significant declines in honey bee populations and even the collapse of entire colonies [65], [66]. As honey bees are important pollinators for many crops, these declines can also have negative impacts on agricultural productivity and ecosystem health.

A 3D model of a Varroa mite and western honey bee (*Apis mellifera*), known as the digital twin [8], [67], [68], has been created, and their electrical properties (*cf.* Fig 28) have been incorporated. Fig. 32 depicts a realistic 3D model of the Varroa mite used in the study, while Fig. 33 shows the 3D model

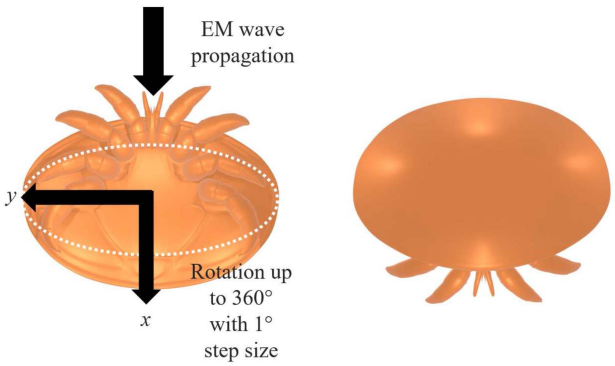

FIGURE 32. The ventral (left) and dorsal (right) views of a Varroa mite.

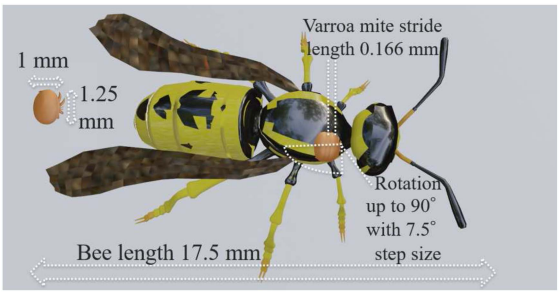

FIGURE 33. Demonstration of the micro-motion of Varroa mite (dorsal view) on its host bee.

depicting the position of the Varroa mite on the host bee. The study also takes into account the random roughness of the insects when they are exposed to THz frequencies, since the physical features of the insect's body become rough at these frequencies. The Beckmann-Kirchhoff (B-K) model has been used to simulate the relative backscatter power from the insect (mite), with the simulation relying on scattered power rather than specular power [69]. The transceiver (TRX) and insect (mite) are positioned 0.2 m apart.

The simulations are performed using a TRX horn that operates at a carrier frequency of 300 GHz. The transmit output power is 0 dBm. Additional information about the specific horn used can be found in [70], [71]. To provide an overview of the simulation approach, three different scenarios are employed and summarized below:

- **Scenario I:** As part of this first scenario, simulations are conducted to record the relative backscatter power while rotating the mite in 1° increments, starting at 0° and ending at 360°.
- **Scenario II:** In the second scenario, simulations are conducted to record the relative backscatter power while rotating the mite in 7.5° increments. This is done with and without the hosting bee, starting at 0° and ending at 90°. A total of 13 steps are recorded and compared.
- **Scenario III:** During the third scenario, the mite undergoes 13 rotations, and during each rotation, three walking steps are taken, with a stride length of $\lambda/6$ or 0.166 mm, to record the relative backscatter power.

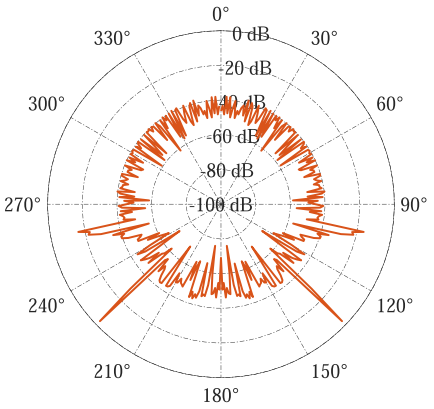

FIGURE 34. PRT-simulated relative backscatter power of a full 3D mite model recorded in a monostatic geometry for different rotation angles at 300 GHz (*Scenario I*).

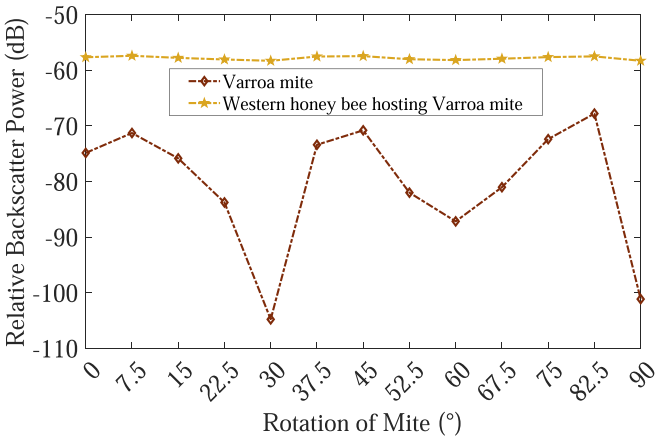

FIGURE 35. Relative backscatter power for 13 rotation steps (*Scenario II*) of a full 3D mite model in its initial position.

B. THZ RAY-TRACING SIMULATION RESULTS

Backscattering of EM waves relies mainly on the body roughness in insects, the angle of incidence, the complex refractive index of insects, and the wavelength involved. When it comes to THz frequencies, the roughness of the body tends to be more prominent, which leads to a significantly stronger backscatter factor. The effect of the mite's rough body on T-rays is examined in ray-tracing simulations by rotating the mite, and the findings are illustrated in the Figs. 34–36.

Fig. 34 depicts the ratio of the power of backscattered signals to the power of transmitted signals of a full 3D mite model. The ray-tracing simulations are conducted at 1° intervals using a monostatic configuration and a carrier frequency of 300 GHz. It is worth noting that the results obtained from the 0° to 360° rotation do not include the host bee. As can be acquired from Fig. 34, the rough surface of the mite model causes incident, reflection, and scattering angles to vary randomly across its body, and some rotational positions produce comparatively stronger backscatter power from the mite. The mite model used is symmetric in terms of its body halves, and

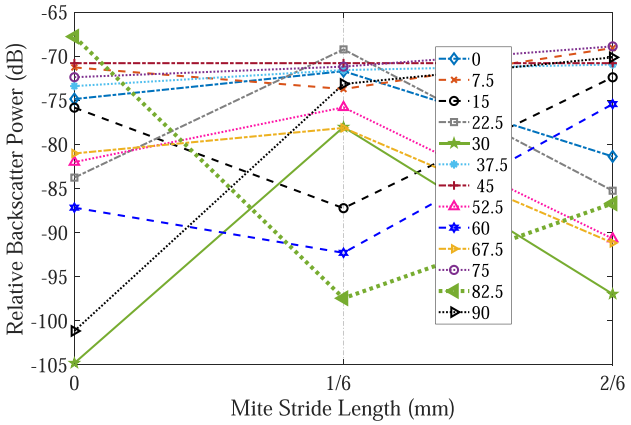

FIGURE 36. Recorded relative backscatter power from a walking mite with a stride length of $\lambda/6$ or 0.166 mm (*Scenario III*).

this characteristic is also evident in the outcomes. As such, an azimuth angle of 101° corresponds to its symmetrical angle of 259°, with a relative backscatter power of -42.89 dB. Similarly, an azimuth angle of 134° corresponds to its symmetrical angle of 226°, with a relative backscatter power of -29.72 dB. The aforementioned results correspond to *Scenario I*.

Further, in Fig. 35, the PRT simulation results for *Scenario II* are illustrated. Regardless of whether the Varroa mite is alone or on a host bee, it assumes the same posture, and this is worth noting. In other words, the orientation of the Varroa mite is consistent when conducting THz ray-tracing simulations for both cases. It is evident that the rotation of the Varroa mite can be readily differentiated in the presence and absence of a host bee. As expected, in the presence of a host bee, the RCS is increased which results in enhanced relative backscatter power. The reason for this is that the bee, being larger in size and having a higher RCS, has a greater influence on the overall RCS with respect to the mite contribution. However, when considering only the Varroa mite, even slight rotational variations have a significant impact on the backscattered power. It is worth noting that the level of detail in the digital twin and the details of the mite's anatomical structure contribute to this variation in power. As such, even minor alterations in orientation towards the transceiver (TRX) appear to be noticeable in these power results. The average relative backscattered power recorded in the presence of host bee is −57.49 dB. In contrast, when considering the Varroa mite alone, the average decrease in relative backscatter power is 18.53 dB. The findings emphasize that 3D photorealistic THz ray-tracing is a fortunate choice for sensing the rotation of small objects like the Varroa mite.

Next, the *Scenario III* results are presented in Fig. 36. This scenario is more advanced and intricate, as it exhibits the combined effects of rotation and stride length. The Varroa mite follows a linear trajectory with a step size of $\lambda/6$ mm, indicating micro-motions that are a fraction of the chosen wavelength. It is noteworthy that the movement occurs perpendicular to the direction of EM wave propagation. We observed that the backscattered power, which is dependent on the mite's body structure, changes with every step and rotation. Interestingly, we noticed a significant decrease in backscattered power for the same rotation but different steps. For instance, when the mite is at its initial location (i.e., first step) and rotated at 82.5°, the backscattered power recorded is −67.78 dB. However, at $\lambda/6$ mm location, the power decreased significantly to −97.44 dB. Our simulation results demonstrate that the micro-motion of the Varroa mite can be accurately captured using 3D PRT simulation. No doubt, the employed PRT is a reliable tool for THz sensing of micro-motion in creatures within this wavelength range. Thus, it can provide initial models for studying THz sensing in conditions where measuring insects can be quite challenging.

X. CONCLUSIONS AND OUTLOOK

Pooya Alibeigloo, Christian Preuss, Enes Mutlu, Robin Kress, Simone Clochiatti, Nils G. Weimann

To have THz sensors for water content and plant growth monitoring, which can play a role in future smart farming and precision agriculture, we aim to develop and use our low-cost, compact-size, battery-driven, robust electronic RTD transceivers. Our future envisioned approach is to utilize and integrate such tiny chips deployed in the field with a cellular wireless network for localized control of the health and water content in plants to achieve a smart farming management system based on distributed plant monitoring [32].

Benedikt Sievert, Marvin Degen, Fabian Brix, Ute Krämer, Daniel Erni, Andreas Rennings

To exploit the full potential of non-invasive THz plant monitoring, the mutual interactions between the different scattering elements in the plant's stem must be taken into account. We address this challenging inverse scattering analysis by combining a very efficient semi-analytical full-wave model with a tailored meassurement setup.

Aman Batra, Fabian Brix, Fawad Sheikh, Andreas Prokscha, Ute Krämer, Thomas Kaiser

Regards to the VNA-based THz imaging results, a 3D high-resolution environment focusing on plants and insects is mapped at a distance of 37 cm. Due to the available high spatial resolution, the three main body parts of the honey bees are well observed. Moreover, the plant leaves in an aphid-infested and an uninfested healthy state are considered. It is observed that the scattering behavior from both leaf surfaces differs and it can be utilized to distinguish between them. Besides, a SAR 3D cube has the potential to provide wide information related to the health of the plant such as water content, and infestation classification by analyzing the leaf-layered structure and presence of insects.

Ingrid Ullmann, Konstantin Root, Martin Vossiek

We demonstrated capturing insect movement with a millimeter-wave imaging radar successfully. Once MIMO radars in the THz range are technologically available, it can be possible the capture movements of much smaller insects. In future research, a more elaborate signal processing strategy for eliminating the background reflection will have to be

investigated along with the hardware. At present, insect movement can be captured, however, sensing of stationary insects is not possible with the employed background suppression technique. For real-world applications however, it is necessary to account for both moving and stationary insects.

Tobias Kubiczek, Jan C. Balzer

We have shown that the broadband RCS of bees can be determined using THz-TDS. The high bandwidth of the THz-TDS system enables broadband RCS characterization of insects, which can be used for insect radar. Further investigations include repeating the measurement for different antenna positions and rotating the insect not only in azimuth, but in azimuth and elevation. This allows for view-independent characterization of insects with radar.

Kevin Kolpatzeck, Jan C. Balzer

THz harmonic radar is a promising approach for tracking of insects in highly scattering environments. For example, the moderate transmission loss of honeycombs at the lower end of the THz range – particularly at frequencies below 200 GHz – can make it possible to follow the path of a bee carrying a nonlinear tag inside the bee hive in real time. The development of highly sensitive harmonic radar for the THz range is a compelling research topic that requires contributions from several different fields of THz science. Areas of interest include the development of high-power transmitters and sensitive harmonic receivers, the design of small and efficient nonlinear tags, the investigation of suitable beam steering concepts, as well as the development of signal processing solutions for robust real-time tracking.

Mandana Jalali, Jan Taro Svejda, Daniel Erni

Our further modeling efforts will focus on the material characterization at THz frequencies of specific bee parts, namely the wings, the cuticula, and the internal parts of the bee. In collaboration with entomologists, it will be necessary to decide which organs (e.g., gastrointestinal tract, visual and ventral nerve cords, etc.) are most important for evaluating the impact of EM energy intake and must in the following be included into an inhomogeneous version of the bee model. In perspective, such a functionalized digital twin could be suitable to predict/explain EM-induced stress as well as provide a reliable tool for developing realistic and highly selective bee monitoring scenarios.

Fawad Sheikh, Andreas Prokscha, Aman Batra, Dien Lessy, Baha Salah, Thomas Kaiser

The 3D photorealistic ray-tracer can efficiently simulate complex sensing scenarios involving intricate objects, making it a valuable tool for sensing living organisms at THz frequencies. However, to achieve accurate results in ray-tracing, it is necessary to build and employ surface-based models since insects are not empty hulls or homogeneous solids. These surface-based models take into account the internal anatomical structures. Currently, the 3D morphable model is used to describe the variation of insect body shapes, and the same homogeneous properties are applied to the entire body of both Varroa mite and western honey bee. Therefore, additional measurements of insects' dielectric properties are required to validate the current approach. Nevertheless, the next step in the PRT simulation involves introducing different dielectric properties for each insect body part in the sensing scenario. This approach will lead to the development of an adaptive backscattering model and enable the sensing of insect populations from afar through machine learning.

The authors listed have come together and are committed to collaborative research aimed at achieving the goal of miniaturizing THz systems for future environmental monitoring applications.

ACKNOWLEDGMENT

The authors also express our gratitude for the valuable collaborative discussions and assistance provided by the members of several institutions including the Institute of Digital Signal Processing (DSV, UDE), Laboratory for General and Theoretical Electrical Engineering (ATE, UDE), Department of High Frequency Electronic Components (BHE, UDE), the Chair of Communication Systems (NTS, UDE), Institute of Microwaves and Photonics (LHFT, FAU) and Institute of Molecular Genetics and Physiology of Plants (MGPP, RUB). Lastly, we express our gratitude to the anonymous reviewers for their diligent scrutiny of our manuscript and for offering numerous perceptive comments and recommendations.

REFERENCES

[1] A. Garcia-Molina and A. Leister, "Accelerated relaxation of photoprotection impairs biomass accumulation in Arabidopsis," *Nature Plants*, vol. 6, no. 2, pp. 9–12, Jan. 2020.

[2] K. Lee et al., "Lack of FIBRILLIN6 in Arabidopsis thaliana affects light acclimation and sulfate metabolism," *New Phytologist*, vol. 225, no. 4, pp. 1715–1731, Feb. 2020.

[3] P. J. Flood et al., "Phenomics for photosynthesis, growth and reflectance in Arabidopsis thaliana reveals circadian and long-term fluctuations in heritability," *Plant Methods*, vol. 12, no. 4, Feb. 2016, Art. no. 14.

[4] S. Rasmussen et al., "Transcriptome responses to combinations of stresses in Arabidopsis," *Plant Physiol.*, vol. 161, no. 4, pp. 1783–1794, Feb. 2013.

[5] S. I. Zandalinas et al., "The impact of multifactorial stress combination on plant growth and survival," *New Phytologist*, vol. 230, no. 3, pp. 1034–1048, May 2021.

[6] S. I. Zandalinas, Y. Fichman, A. R. Devireddy, and R. Mittler, "Systemic signaling during abiotic stress combination in plants," *Proc. Nat. Acad. Sci.*, vol. 117, no. 24, pp. 13810–13820, May 2021.

[7] N. H. D. Olivas et al., "Effect of prior drought and pathogen stress on Arabidopsis transcriptome changes to caterpillar herbivory," *New Phytologist*, vol. 210, no. 4, pp. 1344–1356, Jun. 2016.

[8] F. Sheikh et al., "THz measurements, antennas, and simulations: From the past to the future," *IEEE J. Microwaves*, vol. 3, no. 1, pp. 289–304, Jan. 2023.

[9] F. Sheikh, Y. Gao, and T. Kaiser, "A study of diffuse scattering in massive MIMO channels at terahertz frequencies," *IEEE Trans. Antennas Propag.*, vol. 68, no. 2, pp. 997–1008, Feb. 2020.

[10] P. Hillger, J. Grzyb, R. Jain, and U. R. Pfeiffer, "Terahertz imaging and sensing applications with silicon-based technologies," *IEEE Trans. THz Sci. Technol.*, vol. 9, no. 1, pp. 1–19, Jan. 2019.

[11] S. Wu et al., "Terahertz 3-D imaging for non-cooperative on-the-move whole body by scanning MIMO-array-based Gaussian fan-beam," *IEEE Trans. Antennas Propag.*, vol. 70, no. 12, pp. 12147–12162, Dec. 2022.

[12] J. Wang, S. Zhu, Y. Lin, S. Svanberg, and G. Zhao, "Mosquito counting system based on optical sensing," *Appl. Phys. B, Lasers Opt.*, vol. 126, no. 2, pp. 1–10, Feb. 2020.

[13] Y. Sun, Y. Lin, G. Zhao, and S. Svanberg, "Identification of flying insects in the spatial, spectral, and time domains with focus on mosquito imaging," *Sensors*, vol. 21, May 2021, Art. no. 3329.

[14] Z. Song et al., "Application of lidar remote sensing of insects in agricultural entomology on the chinese scene," *J. Appl. Entomology*, vol. 144, no. 3, pp. 161–169, Apr. 2020.

[15] H. M. Aumann, "A technique for measuring the RCS of free-flying honeybees with a 24 GHz CW doppler radar," in *Proc. IEEE 12th Eur. Conf. Antennas Propag.*, London, U.K., 2018, pp. 1–4.

[16] S. Kong et al., "Insect multifrequency polarimetric radar cross section: Experimental results and analysis," *IEEE Trans. Geosci. Remote Sens.*, vol. 59, no. 8, pp. 6573–6585, Aug. 2021.

[17] P. Hillger et al., "Toward mobile integrated electronic systems at THz frequencies," *IEEE J. Infrared, Millimeter, THz Waves*, vol. 41, pp. 846–869, Jun. 2020.

[18] J. L. Hesler, H. Xu, A. Brissette, and W. L. Bishop, "Development and characterization of THz planar schottky diode mixers and detectors," in *Proc. 19th Int. Symp. Space THz Technol.*, 2008, pp. 224–225.

[19] M. Feiginov, C. Sydlo, O. Cojocari, and P. Meissner, "Resonant-tunnelling-diode oscillators operating at frequencies above 1.1 THz," *Appl. Phys. Lett.*, vol. 99, no. 23, Dec. 2011, Art. no. 233506.

[20] Y. Koyama, R. Sekiguchi, and T. Ouchi, "Oscillations up to 1.40 THz from resonant-tunneling-diode-based oscillators with integrated patch antennas," *Appl. Phys. Exp.*, vol. 6, no. 6, May 2013, Art. no. 064102.

[21] T. Maekawa, H. Kanaya, S. Suzuki, and M. Asada, "Oscillation up to 1.92 THz in resonant tunneling diode by reduced conduction loss," *Appl. Phys. Exp.*, vol. 9, no. 2, Jan. 2016, Art. no. 024101.

[22] R. Izumi, S. Suzuki, and M. Asada, "1.98 THz resonant-tunneling-diode oscillator with reduced conduction loss by thick antenna electrode," in *Proc. IEEE 42nd Int. Conf. Infrared, Millimeter, THz Waves*, Cancun, Mexiko, 2022, pp. 1–2.

[23] M. Feiginov, "Frequency limitations of resonant-tunnelling diodes in sub-THz and THz oscillators and detectors," *J. Infrared, Millimeter, THz Waves*, vol. 40, pp. 365–394, Mar. 2019.

[24] T. Nakagawa, H. Imamoto, T. Kojima, and K. Ohta, "Observation of resonant tunneling in AlGaAs/GaAs triple barrier diodes," *Appl. Phys. Lett.*, vol. 49, no. 2, pp. 73–75, Jul. 1986.

[25] K. Arzi et al., "Triple-barrier resonant-tunnelling diode THz detectors with on-chip antenna," in *Proc. 12th German Microw. Conf.*, Stuttgart, Germany, 2019, pp. 17–19.

[26] K. Arzi et al., "Broadband detection capability of a triple barrier resonant tunneling diode," in *Proc. 2nd Int. Workshop Mobile THz Syst.*, Bad Neuenahr, Germany, 2019, pp. 1–4.

[27] S. Clochiatti, E. Mutlu, C. Preuss, R. Kress, W. Prost, and N. Weimann, "Broadband THz detection using InP triple-barrier resonant tunneling diode with integrated antenna," in *Proc. IEEE 4th Int. Workshop Mobile THz Syst.*, Essen, Germany, 2021, pp. 1–5.

[28] H. B. Zhang, K. Mitobe, and N. Yoshimura, "Application of terahertz imaging to water content measurement," *Jpn J. Appl. Phys.*, vol. 47, no. 10R, Oct. 2008, Art. no. 8065.

[29] R. Gente et al., "Determination of leaf water content from terahertz time-domain spectroscopic data," *IEEE J. Infrared, Millimeter, THz Waves*, vol. 34, pp. 316–323, Mar. 2013.

[30] R. Gente et al., "Outdoor measurements of leaf water content using THz quasi time-domain spectroscopy," *IEEE J. Infrared, Millimeter, THz Waves*, vol. 39, pp. 943–948, Jul. 2018.

[31] E. Castro-Camus, M. Palomar, and A. Covarrubias, "Leaf water dynamics of Arabidopsis thaliana monitored in-vivo using terahertz time-domain spectroscopy," *Sci. Rep.*, vol. 3, Oct. 2013, Art. no. 2910.

[32] M. A. Imran, S. Hussain, and Q. A. Abbasi, "Application of terahertz sensing at nano-scale for precision agriculture," in *Wireless Automation as an Enabler for the Next Industrial Revolution*. Hoboken, NJ, USA: Wiley, 2020, pp. 241–257, doi: 10.1002/9781119552635.ch11.

[33] A. Zahid et al., "Terahertz characterisation of living plant leaves for quality of life assessment applications," in *Proc. Baltic URSI Symp.*, Poznan, Poland, 2018, pp. 117–120.

[34] J. W. Kadereit, C. Körner, P. Nick, and U. Sonnewald, *Strasburger - Lehrbuch Der Pflanzenwissenschaften*. Berlin/Heidelberg, Germany: Springer Spektrum, 2021.

[35] P. Sitte, E. Weiler, J. W. Kadereit, A. Bresinsky, and C. Körner, *Lehrbuch der Botanik für Hochschulen*, 35th ed. Heidelberg, Germany: Spektrum Akademischer Verlag, 2002.

[36] J. Quintana et al., "Root-to-shoot iron partitioning in Arabidopsis requires IRON-REGULATED TRANSPORTER1 (IRT1) protein but not its iron(II) transport function," *Plant J.*, vol. 109, no. 4, pp. 992–1013, Feb. 2022.

[37] P. C. Waterman, "Matrix formulation of electromagnetic scattering," *Proc. IEEE*, vol. 53, no. 8, pp. 805–812, Aug. 1965.

[38] M. Degen et al., "Efficient analysis of the scattering from randomly distributed obstacles using a novel recursive aggregated centered t-matrix algorithm," submitted for publication.

[39] B. Stout, J. -C. Auger, and J. Lafait, "A transfer matrix approach to localfield calculations in multiple-scattering problems," *J. Mod. Opt.*, vol. 49, no. 13, pp. 2129–2152, Nov. 2002.

[40] G. N. Watson, *A Treatise on the Theory of Bessel Functions*, 2nd ed. Cambridge, U.K.: Cambridge Univ. Press, 1966.

[41] A. Batra et al., "Short-range SAR imaging from GHz to THz waves," *IEEE J. Microwaves*, vol. 1, no. 2, pp. 574–585, Apr. 2021.

[42] Y. Sun and D. L. Parker, "Performance analysis of maximum intensity projection algorithm for display of MRA images," *IEEE Trans. Med. Imag.*, vol. 18, no. 12, pp. 1154–1169, Dec. 1999.

[43] J. R. Riley, "Radar cross section of insects," *Proc. IEEE*, vol. 73, no. 2, pp. 228–232, Feb. 1985.

[44] O. Alzaabi et al., "Numerical modeling and measurement of Apis mellifera radar scattering properties," *IEEE Geosci. Remote Sens. Lett.*, vol. 19, 2021, Art. no. 3503205.

[45] L. Dall'Asta and G. Egger, "Preliminary results from beehive activity monitoring using a 77 GHz FMCW radar sensor," in *Proc. IEEE Int. Workshop Metrol. Agriculture Forestry*, Trento-Bolzano, Italy, 2021, pp. 1–6.

[46] J. C. Balzer et al., "THz systems exploiting photonics and communications technologies," *IEEE J. Microwaves*, vol. 3, no. 1, pp. 268–288, Jan. 2023.

[47] D. Damyanov et al., "High resolution lensless terahertz imaging and ranging," *IEEE Access*, vol. 7, pp. 147704–147712, 2019.

[48] D. Damyanov, T. Kubiczek, K. Kolpatzeck, A. Czylwik, T. Schultze, and J. C. Balzer, "3D THz-TDS SAR imaging by an inverse synthetic cylindrical aperture," *IEEE Access*, vol. 11, pp. 9680–9690, 2023.

[49] J. R. Riley et al., "Harmonic radar as a means of tracking the pheromone-finding and pheromone-following flight of male moths," *J. Insect Behav.*, vol. 11, pp. 287–296, Mar. 1998.

[50] E. A. Capaldi et al., "Ontogeny of orientation flight in the honeybee revealed by harmonic radar," *Nature*, vol. 403, no. 6769, pp. 537–540, Feb. 2000.

[51] J. L. Osborne et al., "A landscapescale study of bumble bee foraging range and constancy, using harmonic radar," *J. Appl. Ecol.*, vol. 36, no. 4, pp. 519–533, Dec. 2001.

[52] M. E. O'Neal, D. A. Landis, E. Rothwell, L. Kempel, and D. Reinhard, "Tracking insects with harmonic radar: A case study," *Amer. Entomologist*, vol. 50, no. 4, pp. 212–218, Oct. 2004.

[53] E. T. Cant, A. D. Smith, D. R. Reynolds, and J. L. Osborne, "Tracking butterfly flight paths across the landscape with harmonic radar," *Proc. Roy. Soc. B, Biol. Sci.*, vol. 272, no. 1565, pp. 785–790, Apr. 2005.

[54] R. Maggiora, M. Saccani, D. Milanesio, and M. Porporato, "An innovative harmonic radar to track flying insects: The case of Vespa Velutina," *Sci. Rep.*, vol. 9, no. 1, Aug. 2019, Art. no. 11964.

[55] J. R. Riley and A. D. Smith, "Design considerations for an harmonic radar to investigate the flight of insects at low altitude," *Comput. Electron. Agriculture*, vol. 35, no. 2/3, pp. 151–169, Aug. 2002.

[56] A. Noskov, J. Bendix, and N. Friess, "A review of insect monitoring approaches with special reference to radar techniques," *Sensors*, vol. 21, no. 4, Feb. 2019, Art. no. 1474.

[57] M. Mulot, T. Kroeber, M. Gossner, and J. Froehlich, "Wirkung von nichtionisierender Strahlung (NIS) auf Arthropoden," report commissioned by the Bundesamts für Umwelt (BAFU), Neuenburg, Switzerland, 2022. Accessed: Mar. 22, 2023. [Online]. Available: https://www.emf-portal.org/de/article/49665

[58] International Commission on Non-Ionizing Radiation Protection, "Guidelines for limiting exposure to electromagnetic fields (100KHz-300 GHz)," *Health Phys.*, vol. 118, no. 5, pp. 483–524, May 2020, doi: 10.1097/HP.0000000000001210.

[59] G. Papa et al., "The Honey Bee Apis mellifera: An insect at the interface between human and ecosystem health," *Biology*, vol. 11, no. 2, Feb. 2022, Art. no. 233.

[60] D. Mirkovic, P. M. Stepanian, C. E. Wainwright, D. R. Reynolds, and M. H. M. Menz, "Characterizing animal anatomy and internal composition for electromagnetic modelling in radar entomology," *Remote. Sens. Ecol. Conservation*, vol. 5, no. 2, pp. 169–179, Jun. 2019.

[61] A. Thielens, M. K. Greco, L. Verloock, L. Martens, and W. Joseph, "Radio-frequency electromagnetic field exposure of Western Honey Bees," *Sci. Rep.*, vol. 10, Jan. 2020, Art. no. 461.
[62] A. Thielens, D. Bell, D. B. Mortimore, M. K. Greco, L. Martens, and W. Joseph, "Exposure of insects to radio-frequency electromagnetic fields from 2 to 120 GHz," *Sci. Rep.*, vol. 8, Mar. 2018, Art. no. 3824.
[63] S. Mustafa, A. M. Abbosh, and P. T. Nguyen, "Modeling human head tissues using fourth-order Debye model in convolution-based three-dimensional finite-difference time-domain," *IEEE Trans. Antennas Propag.*, vol. 62, no. 3, pp. 1354–1361, Mar. 2014.
[64] The Mobile THz Company UG, "Photorealistic THz ray-tracer," 2023. [Online]. Available: http://www.themobilethzcompany.com
[65] F. Posada-Florez et al., "Varroa destructor mites vector and transmit pathogenic honey bee viruses acquired from an artificial diet," *PLoS One*, vol. 15, no. 11, Nov. 2020, Art. no. e0242688.
[66] A. Noël, Y. L. Conte, and F. Mondet, "Varroa destructor: How does it harm Apis mellifera honey bees and what can be done about it?," *Emerg. Topics Life Sci.*, vol. 4, no. 1, pp. 45–57, Jul. 2020.
[67] A. Prokscha, F. Sheikh, D. Lessy, N. A. Ali, and T. Kaiser, "Multidisciplinary data fusion for THz ray-tracing," in *Proc. 16th Eur. Conf. Antennas Propag.*, Madrid, Spain, 2022, pp. 1–5.
[68] A. Prokscha, F. Sheikh, D. Lessy, and T. Kaiser, "Portable device-centric human postures for modeling reliable THz channels," in *Proc. IEEE 5th Int. Workshop Mobile THz Syst.*, Duisburg, Germany, 2022, pp. 1–5.
[69] F. Sheikh and T. Kaiser, "A modified Beckmann-Kirchhoff scattering model for slightly rough surfaces at terahertz frequencies," in *Proc. IEEE Int. Symp. Antennas Propag. USNC-URSI Radio Sci. Meeting*, Atlanta, GA, USA, 2019, pp. 2079–2080.
[70] F. Sheikh, B. Salah, D. Lessy, and T. Kaiser, "Unexplored aspects in THz ray-tracing," in *Proc. IEEE 4th Int. Workshop Mobile THz Syst.*, Essen, Germany, 2021, pp. 1–6.
[71] F. Sheikh et al., "Scattering and roughness analysis of indoor materials at frequencies from 750 GHz to 1.1 THz," *IEEE Trans. Antennas Propag.*, vol. 69, no. 11, pp. 7820–7829, Nov. 2021.

FAWAD SHEIKH (Member, IEEE) received the Dr.-Ing. degree from the University of Duisburg-Essen, Duisburg, Germany, in 2019. He is currently a Senior Postdoctoral Researcher with the Institute of Digital Signal Processing (DSV). From 2006 to 2011, he worked on cellular and IT service management projects with Fraunhofer IMS, Duisburg, Germany, KlickTel AG, Essen, Germany, Vodafone D2 GmbH, Düsseldorf, Germany, and Deutsche Telekom AG, Bonn, Germany. From January 2012 to May 2017, he was associated with DSV, University of Duisburg-Essen, for the project Wireless 100 Gb/s and beyond. Since June 2017, he has been with project Mobile MAteRIal TranscEiver. He is a Coordinator of the IEEE International Workshop Series on Mobile Terahertz Systems started in 2018 and the CEO of The Mobile THz Company UG, offering concept designs and performance analyses of Mobile THz Systems. His research interests include systems and components in THz band communications, measurement and modeling of mobile radio channels, massive MIMO systems, mobile material characterization and localization, and THz sensing for monitoring plants, fruits as well as insects within the frequency range of 250 GHz to 5 THz.

ANDREAS PROKSCHA (Graduate Student Member, IEEE) received the M.Sc. degree in electrical engineering from the University of Duisburg-Essen, Duisburg, Germany, in 2019. He is currently working toward the Ph.D. degree with the Institute of Digital Signal Processing (DSV). Since 2020, he has been with ID4us GmbH, Duisburg, Germany, RFID Centric Company. In 2021, he joined DSV. Since June 2021, he has been involved in multiple research projects with main focus on the project mobile MAteRIal TranscEiver. His research interests include 3D environment modeling with applying human kinematics based on inertial sensors, investigating human digital twins within THz communication channels and human medical related applications in millimeter, and THz frequencies.

AMAN BATRA received the B.Tech. degree in electronics and communication engineering from Maharshi Dayanand University, Rohtak, India, in 2014, the M.Sc. degree in embedded systems engineering and the Dr.-Ing. degree from the University of Duisburg-Essen (UDE), Duisburg, Germany, in 2017 and 2021, respectively. He is currently a Postdoctoral Researcher with the Institute of Digital Signal Processing, UDE. He is working on Terahertz and Millimeter Wave radar imaging for environmental and biomedical applications. His research interests include digital signal processing, electromagnetic simulations, and measurements, hardware-software codesign, computer vision, and high-performance computing. He is also a part of the organizing committee of the IEEE IWMTS series.

DIEN LESSY (Graduate Student Member, IEEE) received the B.E. degree in communication engineering from the Electronic Engineering Polytechnic Institute of Surabaya, Surabaya, Indonesia, in 2009, and the M.Sc. degree in computer science and communication engineering from the University of Duisburg Essen, Duisburg, Germany, in 2018. He is currently working on MARIE Project with the Department of Digital Signal Processing, University Duisburg Essen, Germany.

BAHA SALAH (Graduate Student Member, IEEE) received the bachelor's degree in telecommunications engineering from Arab American University, Jenin, Palestine, in 2012, and the master's degree in communications engineering from the University of Duisburg-Essen (UDE), Duisburg, Germany, in 2019. He is currently a Research Assistant with the Department of Digital Signal Processing, UDE. His research interests include time-variant channel estimation for indoor and urban scenarios, the potential applications of THz technology, and incorporating realistic and kinetic 3D modeling for more precise simulation outcomes.

BENEDIKT SIEVERT (Member, IEEE) was born in Krefeld, Germany. He received the B.Sc. and M.Sc. degrees in electrical engineering/high-frequency systems from the University of Duisburg-Essen (UDE), Duisburg, Germany, in 2017 and 2019, respectively. Since 2017, he has been a member of the Laboratory of General and Theoretical Electrical Engineering, UDE. His research interests include mm-wave on chip-antennas, electromagnetic metamaterials, and theoretical and computational electromagnetics applied to mm-wave and THz.

MARVIN DEGEN was born in Speyer, Germany in 1997. He received the B.Eng. degree in electrical engineering from Cooperative State University Baden-Wuerttemberg, Mannheim, Germany, in 2019, and the M.Sc. degree in electrical engineering and information technology from the University of Duisburg-Essen, Duisburg, Germany, in 2022. From 2019 to 2021, he was a Planning Engineer for energy infrastructure projects. Since 2022, he has been a Member of the Laboratory of General and Theoretical Electrical Engineering, University of Duisburg-Essen. His research interests include theoretical and computational electromagnetics and its application in the manipulation of electromagnetic waves.

ANDREAS RENNINGS (Member, IEEE) received the Dipl.-Ing. and Dr.-Ing. degrees from the University of Duisburg-Essen (UDE), Duisburg, Germany, in 2000 and 2008, respectively. He studied electrical engineering with the UDE. He carried out his diploma work during a stay with the University of California in Los Angeles, Los Angeles, CA, USA. From 2006 to 2008, he was with IMST GmbH, Kamp-Lintfort, Germany, where he was an RF Engineer. Since then, he has been a Senior Scientist and Principal Investigator with the Laboratory for General and Theoretical Electrical Engineering, UDE. His research interests include all aspects of theoretical and applied electromagnetics, currently with a focus on medical applications and on-chip millimeter-wave/THz antennas. He was the recipient of several awards, including a student paper price at the 2005 IEEE Antennas and Propagation Society International Symposium and the VDE-Promotionspreis 2009 for the dissertation.

MANDANA JALALI received the B.Sc. degree from Shahid Chamran University, Ahvaz, Iran, in 2007, and the M.Sc. degree from Shiraz University, Shiraz, Iran, in 2010, and the Ph.D. degree in nano-optics from Shiraz University in collaboration with the University of Duisburg-Essen (UDE), Duisburg, Germany, in 2016. Since 2017, she has been a Postdoctoral Researcher with the Department of General and Theoretical Electrical Engineering, UDE, where she is actively involved both in teaching and research. In 2022, she became the group Leader of the ATE-BioEM Center, to establish and develop the center. Her research interests include light-matter interaction, plasmonics, nano optics, optical biosensors, quantum optics, bioelectromagnetics, numerical simulation, computational electromagnetics, and THz based environmental monitoring.

JAN TARO SVEJDA (Member, IEEE) received the B.Sc. degree in electrical engineering from the University of Applied Science, Düsseldorf, Germany, in 2008, and the M.Sc.and Dr.-Ing. degrees in electrical engineering and information technology from the University of Duisburg-Essen (UDE), Duisburg, Germany, in 2013 and 2019, respectively, for his research work in the field of X-nuclei based magnetic resonance imaging. He started his electrical engineering career with the University of Applied Science. He is currently a Research Assistant with the Department of General and Theoretical Electrical Engineering, UDE, where he is involved in teaching several lectures and courses mainly in the field of electrical engineering. His research interests include all aspects of theoretical and applied electromagnetics, currently focusing on medical applications, electromagnetic metamaterials, and scientific computing methods.

POOYA ALIBEIGLOO (Graduate Student Member, IEEE) received the bachelor's degree in electrical engineering from the Sharif University of Technology, Tehran, Iran, in 2015, and the master's degree from Tarbiyat Modares University, Tehran, in 2019. Since 2022, he has been a Research Assistant with the Chair of High-Frequency Components (BHE), University of Duisburg-Essen, Duisburg, Germany. His research interests include terahertz sensing and imaging using power efficient electronic devices. He is part of terahertz.NRW Project.

CHRISTIAN PREUSS was born in Moers, Germany. He received the B.Sc. and M.Sc. degrees in electrical engineering and communications in 2018 and 2020, respectively, from the University of Duisburg-Essen, Duisburg, Germany, where he is currently working toward the Ph.D. degree in electrical engineering with the Department of Components for High Frequency Electronics (BHE). His research interests include the development of THz packages for III-V semiconductor devices and heterointegration concepts based on flip-chip bonding technology.

ENES MUTLU (Graduate Student Member, IEEE) born in Essen. He received the Master of Science degree in nanooptoelectronics in 2019 from the University of Duisburg-Essen, Duisburg, Germany, where he is currently working toward the Ph.D. degree with the Department of High Frequency Electronic Devices. His research work is based on the device development of resonant tunneling diodes and oscillator design at mm-Waves. As a part of the SFB/TRR 196, also called MARIE, he focuses on realizing efficient THz emitters with the future aim to investigate in electronic beam steerable THz emitters.

ROBIN KRESS (Graduate Student Member, IEEE) was born in Essen, Germany. He received the B.Sc. and M.Sc. degrees in electrical engineering and communications in 2018 and 2020, respectively, from the University of Duisburg-Essen, Duisburg, Germany, where he is currently working toward the Ph.D. degree with the Department of Components for High Frequency Electronics (BHE). His research interests include THz oscillator developments on base of InP resonant tunneling antennas and their integration into arrays and modules.

SIMONE CLOCHIATTI received the M.Sc. degree in electrical engineering from the Technical University of Denmark, Kongens Lyngby, Denmark, in 2018, with a focus on areas of RF, microwave engineering, and antennas. He is currently working toward the Ph.D. degree in electrical engineering with the Department of Components for High-Frequency Electronics (BHE), University of Duisburg-Essen, Duisburg, Germany. His research interests include the characterization of THz devices and integrated circuits for signal generation and detection, based on resonant tunneling diode (RTD) semiconductor device.

KEVIN KOLPATZECK received the B.S., M.S., and Dr.-Ing. degrees in electrical engineering and information technology from the University of Duisburg-Essen (UDE), Duisburg, Germany, in 2013, 2016, and 2022, respectively. He investigated terahertz time-domain spectroscopy systems driven by monolithic mode-locked laser diodes with UDE. He is currently a Postdoctoral Researcher with the Chair of Communication Systems (NTS), UDE. His research interests include terahertz photonics, beamforming at terahertz frequencies, and the use of terahertz technology in radar applications and non-destructive testing.

TOBIAS KUBICZEK received the bachelor's degree and the master's degree in communication engineering in 2018 and 2020, respectively, from the University of Duisburg-Essen (UDE), Duisburg, Germany, where he is currently working toward the Dr.-Ing. degree in electrical engineering. Since 2020, he has been a Research Assistant with the Chair of Communication Systems, UDE. His research interests include terahertz imaging and signal processing in terms of synthetic aperture radar and material classification with the help of artificial neural networks. Since 2021, he has been a part of the MARIE Project for mobile material characterization and localization by electromagnetic sensing using mobile THz systems.

INGRID ULLMANN (Member, IEEE) received the M.Sc. degree in electrical engineering and the Ph.D. degree from Friedrich-Alexander-Universität Erlangen-Nürnberg (FAU), Erlangen, Germany, in 2016 and 2021, respectively. She is currently a Postdoc and the Head of the research group Wave-based Imaging Systems, Institute of Microwaves and Photonics, FAU. In 2022, she spent one month as a Visiting Researcher with the Microwave Sensing, Signals and Systems Group, Delft University of Technology, Delft, the Netherlands. Her research interests include radar imaging and radar signal processing for nondestructive testing, security screening, medical radar and automotive applications. She is a Reviewer for the European Radar Conference (EuRAD) and various journals in the field of microwaves and is a member of the IEEE CRFID Technical Committee on Motion Capture and Localization. Since 2022, she has been an Associate Editor for IEEE TRANSACTIONS ON RADAR SYSTEMS. Dr. Ullmann was the recipient of the Argus Science Award (sponsored by Airbus Defense and Space, now Hensoldt) in 2016 and EuRAD Conference Prize in 2019.

KONSTANTIN ROOT received the B.Eng. degree in electrical engineering from Ostbayerische Technische Hochschule Regensburg in 2017, and the M.Sc. degree in electrical engineering from Friedrich-Alexander Universität (FAU) Erlangen-Nürnberg, Germany, in 2019. Since 2019, he has been a Research Scientist with the Institute of Microwaves and Photonics, FAU. His research interests include radar signal processing and polarimetric radar imaging.

FABIAN BRIX is currently working toward the bachelor's degree in biology and environmental engineering with Ruhr-University-Bochum, Bochum, Germany. In 2022, he joined the Group of Prof. Ute Krämer Ruhr-University-Bochum, Bochum. His research interests include the application of THz technology in the biology and the influence of electromagnetic waves on plants.

UTE KRÄMER received the D.Phil. degree from the University of Oxford, Oxford, U.K. as a Rhodes Scholar. She is currently a Full Professor with the Ruhr University Bochum, Bochum, Germany, where she holds the Chair of Molecular Genetics and Physiology of Plants. She studies the genetic basis of evolutionary adaptations in plants employing the metal hyperaccumulator species *Arabidopsis halleri* as a model – sometimes in comparison to its close relative *Arabidopsis thaliana*, in which she also addresses fundamental molecular mechanisms of plant metal homeostasis. She is a Member of the German Academy of Sciences Leopoldina and was awarded an Advanced Grant of the European Research Council in 2018.

MARTIN VOSSIEK (Fellow, IEEE) received the Ph.D. degree from Ruhr-Universität Bochum, Bochum, Germany, in 1996. In 1996, he joined Siemens Corporate Technology, Munich, Germany, where he was the Head of the Microwave Systems Group from 2000 to 2003. Since 2003, he has been a Full Professor with Clausthal University, Clausthal-Zellerfeld, Germany. Since 2011, he has been the Chair of the Institute of Microwaves and Photonics (LHFT), Friedrich-Alexander-Universität Erlangen-Nürnberg, Erlangen, Germany. He has authored or coauthored more than 350 articles. His research has led to more than 100 granted patents. His research interests include radar, microwave systems, wave-based imaging, transponders, RF identification, communication, and wireless sensor and locating systems. He is a member of the German National Academy of Science and Engineering (acatech) and of the German Research Foundation (DFG) Review Board. He is a member of the IEEE Microwave Theory and Technology (MTT) Technical Committees for MTT-24 Microwave/mm-wave Radar, Sensing, and Array Systems; MTT-27 Connected and Autonomous Systems (as Founding Chair), and MTT-29 Microwave Aerospace Systems. He also serves on the advisory board of the IEEE CRFID Technical Committee on Motion Capture and Localization. Dr. Martin Vossiek was the recipient of numerous best paper prizes and other awards. In 2019, he was awarded the Microwave Application Award by the IEEE MTT Society (MTT-S) for Pioneering Research in Wireless Local Positioning Systems. Dr. Vossiek has been a member of organizing committees and technical program committees for many international conferences and has served on the review boards of numerous technical journals. From 2013 to 2019, he was an Associate Editor for IEEE TRANSACTIONS ON MICROWAVE THEORY AND TECHNIQUES. Since October 2022, he has been an Associate Editor-in-Chief of IEEE TRANSACTIONS ON RADAR SYSTEM.

JAN C. BALZER (Member, IEEE) received the Dipl.-Ing. (FH) degree in telecommunications from the Dortmund University of Applied Sciences, Dortmund, Germany, in 2008, and the Master of Science degree in electrical engineering and information technology and the Dr.-Ing. degree from Ruhr University Bochum, Bochum, Germany, in 2010 and 2014, respectively. In 2015, he has joined the research group of Prof. Martin Koch, Philipps University of Marburg, Marburg, Germany, as a Postdoctoral Fellow. Since 2017, he has been an Assistant Professor of terahertz systems with the Faculty of Engineering, University of Duisburg-Essen, Duisburg, Germany. His scientific research focuses on ultrafast semiconductor lasers. Then, he moved to the field of terahertz radiation generation and applications. He made contributions in the field of compact laser diode-driven THz systems, 3D printed THz devices, high-resolution THz imaging, and THz material characterization.

NILS G. WEIMANN (Member, IEEE) received the Diploma in physics from the University of Stuttgart, Stuttgart, Germany, in 1996, and the Ph.D. degree in electrical engineering from Cornell University, Ithaca, NY, USA, in 1999. He was a Technical Manager with Alcatel Lucent's Bell Laboratories, Murray Hill, NJ, USA, till 2012. He was leading the InP Devices Laboratory, Ferdinand-Braun-Institute, Berlin, Germany. In 2017, he was appointed as a Full Professor with the University of Duisburg-Essen, Duisburg, Germany, in the faculty of engineering, chairing the department for high frequency components.

THOMAS KAISER (Senior Member, IEEE) received the Diploma in electrical engineering from Ruhr-University Bochum, Bochum, Germany, in 1991, and the Ph.D. (with distinction) and German Habilitation degrees in electrical engineering from Gerhard Mercator University, Duisburg, Germany, in 1995 and 2000, respectively. From 1995 to 1996, he spent a research leave with the University of Southern California, Los Angeles, Los Angeles, CA, USA, which was grant-aided by the German Academic Exchange Service. From April 2000 to March 2001, he was the Head of the Department of Communication Systems, Gerhard Mercator University, and from April 2001 to March 2002, he was the Head of the Department of Wireless Chips and Systems, Fraunhofer Institute of Microelectronic Circuits and Systems, Duisburg. From April 2002 to July 2006, he was the Co-Leader of the Smart Antenna Research Team, University of Duisburg-Essen (UDE). In 2005, he joined the Smart Antenna Research Group, Stanford University, Stanford, CA, USA, and in the winter of 2007, he joined the Department of Electrical Engineering, Princeton University, Princeton, NJ, USA, as a Visiting Professor. From 2006 to 2011, he was the Head of the Institute of Communication Technology, Leibniz University of Hannover, Hannover, Germany. He is currently the Head of the Institute of Digital Signal Processing, UDE, is the Founder of three start-up companies and CEO of ID4us GmbH and RFID Centric Company. He is the author and coauthor of more than 300 papers in international journals and conference proceedings and two books titled *Ultra Wideband Systems With MIMO* (Wiley, 2010) and *Digital Signal Processing for Passive RFID* (Wiley, 2015) and he is the Speaker of the Collaborative Research Center Mobile Material Characterization and Localization by Electromagnetic Sensing (MARIE). Dr. Kaiser was the founding Editor-in-Chief of the *e-letter* of the IEEE Signal Processing Society and the General Chair of the IEEE International Conference on UltraWideBand in 2008, International Conference on Cognitive Radio Oriented Wireless Networks and Communications in 2009, IEEE Workshop on Cellular Cognitive Systems in 2014, and IEEE Workshop Series on Mobile THz Systems started in 2018.

DANIEL ERNI (Member, IEEE) received the Diploma degree in electrical engineering from the University of Applied Sciences Rapperswil (OST), Rapperswil, Switzerland, in 1986, and the Diploma degree in electrical engineering and the Ph.D. degree in laser physics from ETH Zürich, Zürich, Switzerland, in 1990 and 1996, respectively.

Since 1990, he has been with the Laboratory for Electromagnetic Fields and Microwave Electronics, ETH Zürich. From 1995 to 2006, he was the Founder and the Head of the Communication Photonics Group, ETH Zürich. Since October 2006, he has been a Full Professor with the Laboratory for General and Theoretical Electrical Engineering, University of Duisburg-Essen, Duisburg, Germany. Between 2017 and 2018, he joined the Institute of Electromagnetic Fields (IEF), ETH Zürich, as a Visiting Professor. He is also the Co-Founder of the spin-off company airCode, Duisburg, Germany, working on flexible printed RFID technology. His research interests include optical interconnects, nanophotonics, plasmonics, advanced solar cell concepts, optical and electromagnetic metamaterials, RF, mm-wave and THz engineering, chipless flexible RFIDs, biomedical engineering, bioelectromagnetics, marine electromagnetics, computational electromagnetics, multiscale and multiphysics modeling, numerical structural optimization, and science and technology studies. Dr. Erni is also a Fellow of the Electromagnetics Academy and a member of the Center for Nanointegration Duisburg-Essen, Materials Chain, Flagship Program of the University Alliance Ruhr, the Swiss Physical Society, German Physical Society (DPG), and Optical Society of America (Optica).